Virology 531 (2019) 1–18

Contents lists available at ScienceDirect

Virology

journal homepage: www.elsevier.com/locate/virology

Mosquito cells persistently infected with dengue virus produce viral particles with host-dependent replication

José Manuel Reyes-Ruiz[a], Juan Fidel Osuna-Ramos[a], Patricia Bautista-Carbajal[a], Elizabeth Jaworski[e], Rubén Soto-Acosta[e], Margot Cervantes-Salazar[a], Antonio H. Angel-Ambrocio[b], Juan Pablo Castillo-Munguía[c], Bibiana Chávez-Munguía[a], Mónica De Nova-Ocampo[c], Andrew Routh[e,f], Rosa María del Ángel[a,*], Juan Santiago Salas-Benito[c,d,**]

[a] Departamento de Infectómica y Patogénesis Molecular, Centro de Investigación y de Estudios Avanzados del Instituto Politécnico Nacional, Mexico
[b] División de Investigación, Facultad de Medicina, Universidad Autónoma de México, Mexico
[c] Maestría en Ciencias en Biomedicina Molecular, Escuela Nacional de Medicina y Homeopatía, Instituto Politécnico Nacional, Mexico
[d] Doctorado en Ciencias en Biotecnología, Escuela Nacional de Medicina y Homeopatía, Instituto Politécnico Nacional, Mexico
[e] Department of Biochemistry and Molecular Biology, The University of Texas, Medical Branch, Galveston, TX 77555, USA
[f] Sealy Center for Structural Biology and Molecular Biophysics, The University of Texas Medical Branch, Galveston, TX 77555, USA

ARTICLE INFO

Keywords:
Dengue viruses
Mosquito cells
Persistent viral infection
Viral fitness
Host adaptation

ABSTRACT

Dengue viruses (DENV) are important arboviruses that can establish a persistent infection in its mosquito vector *Aedes*. Mosquitoes have a short lifetime in nature which makes trying to study the processes that take place during persistent viral infections in vivo. Therefore, C6/36 cells have been used to study this type of infection. C6/36 cells persistently infected with DENV 2 produce virions that cannot infect BHK -21 cells. We hypothesized that the following passages in mosquito cells have a deleterious impact on DENV fitness in vertebrate cells. Here, we demonstrated that the viral particles released from persistently infected cells were infectious to mosquito but not to vertebrate cells. This host restriction occurs at the replication level and is associated with several mutations in the DENV genome. In summary, our findings provide new information about viral replication fitness in a host-dependent manner.

1. Introduction

Dengue viruses (DENV) are members of the *Flaviviridae* family and Flavivirus genus that comprises four antigenically distinct serotypes (DENV 1–4) (Islam et al., 2015). DENV particles are ~50 nm in diameter and contains a positive-sense RNA genome of approximately 11 kb with a single open reading frame (ORF) that encodes three structural (C, prM, and E) and seven non-structural (NS1, NS2A, NS2B, NS3, NS4A, NS4B, and NS5) proteins (Gebhard et al., 2011). Factors such as the host cholesterol (Osuna-Ramos et al., 2018) and the structural proteins of the virus participate in the assembly of the virion and in essential processes such as virus attachment, internalization, and morphogenesis, while the non-structural proteins are involved in the replication complexes formation, viral replication, and evasion of the host immune response (Perera and Kuhn, 2008).

DENV are important arboviral pathogens (Bhatt et al., 2013; Stanaway et al., 2016; WHO, 2009) with endemic and epidemic transmission cycles, becoming an important global burden and a growing challenge to public health (Bhatt et al., 2013; Islam et al., 2015). In humans, DENV infection can produce clinical manifestations ranging from a mild fever to dengue shock syndrome (Díaz et al., 1988; Hadinegoro, 2012; Wahid et al., 2000). However, this infection can be acute and self-limiting (Yacoub and Wills, 2014) in contrast with the persistent infection in the cultured mosquito cells as well as in the adult female mosquito vector (Blair, 2011; Blair et al., 2000; Chen et al., 1994; Juárez-Martínez et al., 2013; Kuno, 1982; Sánchez-Vargas et al., 2009). Since arthropods do not have a conventional immunological memory, the persistent infection seems to be a strategy for survival

* Corresponding author.
** Correspondence to: Escuela Nacional de Medicina y Homeopatía, Instituto Politécnico Nacional, Guillermo Massieu Helguera #239, Frac. La Escalera-Ticomán, Mexico City CP 07320, Mexico.
E-mail addresses: rmangel@cinvestav.mx (R.M. del Ángel), jsalas@ipn.mx (J.S. Salas-Benito).

https://doi.org/10.1016/j.virol.2019.02.018
Received 31 August 2018; Received in revised form 22 February 2019; Accepted 26 February 2019
Available online 27 February 2019
0042-6822/

where control over viral replication is maintained (Goic and Saleh, 2012). The mechanisms involved in the establishment and maintenance of persistent infections are poorly understood, but it seems to be a multifactorial process (Salas-Benito and De Nova-Ocampo, 2015).

The adult female mosquito has an average life span of approximately 8.6 days (Focks et al., 1993; Halstead, 2008), this makes trying to study the processes that take place during persistent viral infections in vivo. Thus cellular models have been used instead. Thus, C6/36 cells from *Aedes albopictus* mosquitoes (Igarashi, 1978) have been extensively used as a model to study flavivirus persistent infections (Chen et al., 1994; Dittmar et al., 1982; Igarashi, 1979; Kanthong et al., 2010, 2008; Tsai et al., 2007). In this regard, C6/36 cell line persistently infected with DENV 2, called C6-L cells (Juárez-Martínez et al., 2013), initially released viral particles detectable by plaque assay in BHK-21 cells, but after 42 weeks of culture, the lytic plaques were no longer detectable. Nevertheless, the detection of the viral genome and viral proteins such as NS1, NS5, and E in C6-L cells indicated the presence of DENV (Juárez-Martínez et al., 2013). These results suggested that DENV adaptation in the C6-L mosquito cells could lead to the restriction on viral fitness in vertebrate cells. Thus, we hypothesize that following serial passage in mosquito cells has a deleterious impact on DENV fitness in vertebrate cells, as has been suggested previously (Lee et al., 1997; Filomatori et al., 2017; Vasilakis et al., 2009; Villordo et al., 2015). Although a great deal of information about this subject, the aspects and determinants of the fitness cost associated with host adaptation remain as an object of study. In the present work, the production and infectivity of DENV particles from C6-L cells were analyzed, finding that the viral particles produced and released from C6-L cells can infect mosquito (C6/36 and Aag2 cells) but not mammalian cells (Vero, Huh-7, and BHK-21 cells). This host restriction occurs during the viral replication process since neither viral binding nor viral entry seems to be restricted in mammalian cells, and it could be associated with mutations in the DENV protein-coding regions as well as in their 3′- and 5′-untranslated regions (UTRs). Our studies suggest a host-specific viral adaptation generated during the persistent infection.

2. Material and methods

2.1. Cells and viruses

C6/36 *Aedes albopictus* cells (Igarashi, 1978) were adapted to grow at 35 °C (Kuno and Oliver, 1989), C6-L cells (C6/36 persistently infected with DENV 2) (Juárez-Martínez et al., 2013), and BHK-21 cells were cultured in minimum essential medium (MEM) (Invitrogen) supplemented with 10% fetal bovine serum (FBS), 1X vitamin solution (Invitrogen), 0.034% sodium bicarbonate (J.T. Baker), 100 U/mL penicillin and 100 μg/mL streptomycin (Sigma). Huh-7 cells (kindly donated by Dr. Ana María Rivas, Universidad Autónoma de Nuevo León, Mexico) and Vero cells (Green monkey kidney cells, ATCC CCL-81) were grown in advanced DMEM supplemented with 2 mM glutamine, 5% FBS, fungizone (1 mL/L), penicillin (5×10^4 U/mL), and streptomycin (50 μg/mL) at 37 °C in a 5% CO_2 humidified atmosphere. Aag2, *Aedes aegypti* cells (kindly donated by Dr. Juan Ludert, Cinvestav, Mexico) were maintained at 28 °C in Schneider's *Drosophila* medium with L-glutamine (Gibco, Thermo Fisher Scientific) supplemented with 10% FBS, 100 U/mL penicillin and 100 μg/mL streptomycin (Sigma).

DENV serotype 2 (New Guinea C strain) (kindly donated by the Instituto de Diagnóstico y Referencia Epidemiológicos (InDRE)) was propagated in suckling Balb/c mice as described previously (Gould and Clegg, 1991), and used as a positive control. The virus titer was determined by plaque assay using BHK-21 cells monolayers as described below. Sindbis virus (SINV) (VR-1248 strain-ATCC) was similarly propagated. Brain extracts from uninfected suckling Balb/c mice were used as a control (mock). The virus titer from the C6-L cells was determined by fluorescent focus assay in C6/36 cells.

2.2. Inoculation of suckling mice

Two-day-old Balb/c mice were inoculated intracerebrally through the bregmatic fontanel with 5 μL of culture supernatant from mock-infected cells, DENV 2-infected cells, and C6-L cells, according to a previously described protocol (Gould and Clegg, 1991), and the symptoms and survival were monitored daily.

2.3. Viral infection

The cells were mock-infected, DENV 2-infected (MOI 1), SINV-infected (MOI 1), or treated with viral particles from supernatant from C6-L cells (MOI 1) previously filtered through a 0.22 μm membrane (Millipore), and were subsequently incubated for 2 h at 37 °C with gentle shaking. Then, the monolayers were treated with acid glycine (pH 3) for 30 s to inactivate the non-internalized virus, and the infection was allowed to proceed for 48 h at 35 °C.

2.4. Detection DENV genome by RT-PCR

Total RNA from mock-infected C6/36 cells, C6-L cells, and C6/36 cells acutely infected with DENV 2 was purified using the Trizol reagent (Invitrogen) according to the manufacturer's instructions. The RNA was treated with DNase (New England Biolabs) at 37 °C for 15 min. The amplification of the DENV genome was performed with the DV2M15 5'-TGTTAATGGGTCTTGGGAAAGGATG-3' and DV2M16 5'-TAAGGACTC TGAGTGTTCGTCCTGC-3' primers for the NS4A-NS4B-NS5 region (1,019-bp fragment), and the DV2C-L 5'-CAATATGCTGAAACGCGAGA-3' and DV2C-R 5'-TGCTGTTGGTGGGATTGTTA-3' primers for the C region (151-bp fragment). The RT-PCR Access kit (Promega) and a Mastercycler (Eppendorf) were used as reported previously (Juárez-Martínez et al., 2013). As an internal control, the AegS7F 5'-GGGACA AATCGGCCAGGCTATC-3' and AegS7R 5'-TCGTGGACGCTTCTGCTTG TTG-3') primers were used to amplify the *Aedes aegypti* ribosomal S7 gene (190-bp fragment); Id: AAEL009496-RA. The amplicons were analyzed by 1% agarose gel electrophoresis stained with Gel Red (Biotium) and visualized in a Bio-imaging system Mini Bis Pro (DNS).

2.5. Quantification of the DENV genome by qRT-PCR

The RNA of the supernatant from C6-L cells was purified using the Quick-RNA MicroPrep Kit (Zymo Research) according to the manufacturer's instructions. To amplify the fragment of interest of the viral genome, which correspond to a 151-bp fragment of the DENV capsid gene, a conventional RT-PCR from RNA isolated from mock-infected C6/36 cells, DENV 2-infected C6/36 cells, C6-L cells, and C6/36 cells treated with the supernatant from C6-L cells was performed using the DV2C-L and DV2C-R primers above described. This product was cloned in a pJet1.2 Vector System (Thermo scientific), and the recombinant plasmid was purified and quantified by spectrometry at $\lambda = 260$ nm. A dilution containing 10^{10} copies of plasmid/mL was prepared according to the formula:

$$No.\ Copies = \frac{(6x10^{23} copies/mol)\,(concentration\ [g/\mu L])}{plasmid\ molecular\ weight} + insert\ [g/\mu L]$$

Serial dilutions of the plasmid (10^9–10^2 copies/mL) were prepared, and a standard curve was generated.

The cDNA was obtained by reverse transcription using 1 μg of total RNA from each sample, the enzyme ImpromII (Promega), and the random primers (0.025 μg/μL) (Promega) were added during 1 cycle of amplification under the following conditions: 25 °C for 5 min, 42 °C for 60 min, and 70 °C for 15 min (Veriti Thermal Cycler, Applied Biosystems). The real-time PCR amplification was performed with the SYBR Fast universal kit (Kapa) in an Eco Illumina System apparatus using a reaction mix containing 5 μL of 2X Master Mix and 1 μL of cDNA under

the following conditions: 2 min at 50 °C, 2 min at 95 °C, 40 cycles of 5 s at 95 °C, and 30 s at 55 °C. Finally, a dissociation curve was made by heating of products between 55 °C and 95 °C to confirm primer dimer absence.

2.6. Plaque assay

BHK-21 cells monolayers (2.5×10^5 cells at 90% confluence in 24-well plates) were infected with different dilutions of the supernatant from mock-infected C6/36 cells, DENV 2-infected C6/36 cells, C6-L cells, SINV-infected C6/36 cells, and SINV-infected C6-L cells, for 4 h at 37 °C. Overlay medium (0.5 mL; MEM supplemented with 7.5% FBS, 1% carboxymethylcellulose, and antibiotics) was then added, and the cells were incubated for five days to the case of supernatant from cells infected with DENV and three days to the supernatant from cells infected with SINV, at 37 °C in a 5% CO_2 humidified atmosphere. Finally, the medium was removed, and the monolayers were stained with naphthol blue black (0.1% naphthol blue black, 0.165 M sodium acetate, and 6% acetic acid) for 15 min at room temperature (RT), and the viral yield from three independent experiments was measured and expressed in the log of plaque forming units (PFU)/mL.

2.7. Focus forming assay

C6/36 cells monolayers at 90% confluence in 96-well plates were infected with different dilutions of the supernatant from C6-L cells for 4 h at 37 °C to determine the virus titer from the viral particles. The cells were fixed with 8% formaldehyde, permeabilized for 20 min (0.1% saponin, 1% FBS, and 1X PBS), and incubated for 2 h at RT with mouse anti-prM/E monoclonal antibody (ATCC HB-114). Donkey anti-mouse Alexa 488 (Life Technologies) was used as secondary antibody.

2.8. Detection of intracellular and extracellular viral particles

C6/36 and C6-L cells were seeded into 6-well plates (1×10^6 cells per well), and later, C6/36 cells were infected with DENV 2 at an MOI (multiplicity of infection) of 1, or mock-infected at 37 °C for 2 h with gentle shaking. The inoculum was removed, the cells were washed with acid glycine (pH 3) to inactivate the non-internalized virus, and the infection was allowed to proceed for 48 h at 35 °C. Then, the supernatant (extracellular viral particles) was recovered and filtered through a 0.22 μm membrane (Millipore), and the cell monolayers were treated with acid glycine as described above. The intracellular viral particles were recovered with three freeze-thaw cycles in PBS, and after the removal of the cellular debris by centrifugation at 10,000 rpm for 10 min in a microfuge 5415 R (Eppendorf), the supernatant was recovered. The viral yield from three independent experiments was determined by plaque assays in BHK-21 cell monolayers as described above.

2.9. Transmission electron microscopy (TEM)

C6/36 and C6-L cells were grown in T-75 flasks (Corning). Mock-infected C6/36 cells, C6/36 cells infected with DENV 2 at a MOI of 1, C6-L cells, and C6/36 cells treated with the supernatant from the C6-L cells at a MOI of 1, after 48 h, were fixed with 2.5% glutaraldehyde in 0.1 M sodium cacodylate buffer pH 7.2 for 1 h at RT, and post-fixed with 1% osmium tetroxide for 1 h at RT. The samples were dehydrated through an ethanol gradient and propylene oxide, and then were embedded in Polybed epoxy resins and polymerized at 60 °C for 24 h. Finally, 70-nm thin sections were stained with uranyl acetate and lead citrate and were analyzed using a Jeol JEM-1011 transmission electron microscope (Jeol Ltd., Tokyo, Japan).

2.10. Transmission immunoelectron microscopy (TIM)

C6/36 and C6-L cells were grown in T-75 flasks (Corning). Mock-infected C6/36 cells, C6/36 cells infected with DENV 2 at an MOI of 1, C6-L cells, and C6/36 cells treated with the supernatant from the C6-L cells at an MOI of 1, after 48 h, were fixed with 4% paraformaldehyde/0.5% glutaraldehyde for 1 h at RT. Then, the cells were dehydrated through increasing concentrations of ethanol, embedded in the acrylic resin (LR White), and polymerized under UV irradiation at 4 °C overnight. Resin-embedded cells sections of 70 nm were mounted on Formvar-covered nickel grids and were incubated in PBS with 10% FBS for 1 h to block nonspecific binding, and reacted with an anti-NS3 antibody (Genetex, catalog number 124252) diluted 1:20 in PBS with 5% FBS. The samples were washed three times and incubated with an anti-rabbit IgG secondary antibody conjugated to 20-nm colloidal gold particles (Ted Pella Inc., Redding, CA, USA) at RT for 1 h. Finally, the sections were contrasted with uranyl acetate and lead citrate before being examined under a Jeol JEM-1011 transmission electron microscope (Jeol Ltd., Tokyo, Japan).

2.11. Flow cytometry and confocal microscopy

Mock-infected C6/36 cells, DENV-infected C6/36 cells, C6-L cells, and C6/36 cells treated with the supernatant from C6-L cells were analyzed by flow cytometry to determine the percentage of infected cells, while the viral infection in the mammalian (BHK-21, Vero, and Huh-7 cells) and mosquito cells (C6/36 and Aag2 cells) infected with DENV, mock-infected, or treated with the supernatant from C6-L cells was evaluated by confocal microscopy. The cells were grown in 12-well plates for flow cytometry and on coverslips placed in 24-well plates for confocal microscopy. The cells were fixed with 3% formaldehyde, permeabilized for 20 min (0.1% saponin, 1% FBS, and 1X PBS), and incubated for 2 h at RT with mouse anti-prM/E monoclonal antibody (ATCC HB-114). Donkey anti-mouse Alexa 488 (Life Technologies) was used as secondary antibody, and the nuclei were counterstained with Hoechst (Santa Cruz). The flow cytometry was performed in a BD LSR Fortessa, and the data were analyzed by the FlowJo v.10 software. The slides were observed in a Zeiss LSM700 laser confocal microscopy, and the images were analyzed using the ZEN software, v. 2010.

2.12. Virus binding assay

Huh-7 cells were infected with DENV 2, mock-infected or treated with the supernatant from the C6-L cells in suspension for 30 min at 4 °C. Then, they were fixed with 1% formaldehyde, blocked with 1% FBS, and incubated with mouse anti-DENV 2 monoclonal antibody (MAB8702; Millipore). As a secondary antibody, a donkey anti-mouse Alexa 488 was used (Life Technologies). The percentage of positive cells to DENV 2 was determined by flow cytometry.

2.13. Virus entry assay

Huh-7 cells were incubated with DENV 2, mock-infected or treated with the supernatant from C6-L cells at 4 °C for 5 min to synchronize the infection. Then, the temperature was increased to 37 °C for 1 h to allow virus internalization. The cells were washed with acid glycine to inactivate the noninternalized viral particles. Finally, the samples were analyzed by confocal microscopy and flow cytometry using a rabbit anti-C polyclonal antibody (Genetex, 103343), and goat anti-rabbit Alexa 555 (Life Technologies) as a secondary antibody.

2.14. Western blot

Huh-7 cells were treated with DENV 2, mock or incubated with the supernatant from C6-L cells at 4 °C for 5 min. Then, the temperature was changed to 37 °C for 1 h to allow virus internalization. The cells were washed with acid glycine to inactivate the non-internalized virus and treated with lysis buffer (10 mM Tris-HCl pH 8, 1 mM EDTA, 0.5% deoxycholate, 1 mM EGTA, 1% Triton X-100, 0.1% SDS, and 100 mM NaCl) and protease inhibitor Complete Mini, EDTA-free (Roche) to

obtain total protein extracts. A total of 50 µg of protein were assayed by SDS-PAGE and immunoblotting using a rabbit anti-C polyclonal antibody (Genetex, 103343), and a mouse anti-actin monoclonal antibody (generously donated by Dr. José Manuel Hernández, Cinvestav, Mexico) as a loading control. The proteins were detected using the Super Signal West Femto Chemiluminescent Substrate (Thermo Scientific).

2.15. RNAseq library preparation and data analysis

The viral particle-associated genome from the supernatant from C6-L cells (the passages 30 and 56) was purified using QIAamp Viral RNA Mini Kit (QIAGEN). The genome from the viral particles released after 48 hpi was used for comparison. Purified RNA extracted from DENV particles was prepared for RNAseq analysis using the ClickSeq methodology for library synthesis, as described previously (Jaworski and Routh, 2017; Routh et al., 2015). Briefly, approximately 200 ng of purified viral RNAs without any fragmentation was used as input in a reverse-transcription reaction (SSIII, *Invitrogen*) using manufacturer's protocols with the exception that 3′-azido-nucleotides were supplemented at a ratio of 1:20 AzNTPs to dNTPs. RT was primed using semi-random primers containing six random nucleotides and 34 nts of the Illumina p7 indexing adaptor. Due to the presence of the terminating nucleotides, stochastically terminated azido-blocked cDNA fragments are generated. These were purified away from the other components of the RT reaction using Zymo DNA clean columns and eluted in 50 mM HEPES pH 7.0. 'Click-Ligation' was initiated by adding 5′ hexynyl-functionalized Illumina p5 universal adaptor (*IDT*), followed by vitamin-C reduced 10 mM Cu-TBTA (*lumiprobe*) in 50% DMSO. The click-reaction was allowed to proceed for 30 min, and then the click-ligated cDNA was purified using Zymo DNA clean columns. Finally, the cDNA fragments were PCR amplified in 18 cycles to fill-in the remaining portions of the p7 Illumina adaptor and to add multiplexing barcodes. Final libraries were size selected on 2% agarose gels to 300–600 nucleotides, corresponding to fragment lengths of ~150–450 nts.

Pooled libraries were submitted for sequencing at the UTMB next-generation sequencing core on a NextSeq. 550 acquiring 1 × 150 SE reads. Raw reads trimmed using cutadapt (Martin, 2011) and quality filtered requiring > 98% of the nucleotides to have base-calling PHRED scores > 20. Quality filtered reads were aligned to the Dengue virus-2 NG strain reference sequence using HiSat2 (Kim et al., 2015) and then mismatching nucleotides were found and corrected using the same tools *mpileup* command. After reference correction, this process was iterated increasing the number of mapped reads until no further reads could be mapped and a final reference genome was returned. Final alignments were visualized and inspected using Tablet (Milne et al., 2010) to ensure that genome coverage was even and complete.

2.16. Northern blot targeting 3'-UTR

Total RNA was collected from DENV-infected C6/36 cells or C6-L cells (passage 56) using TRIzol (Invitrogen). Northern blot was performed as previously described (Pompon et al., 2017) using NorthernMax kit (Ambion) and the 5'-CGTTAAAAGAAGTCAGGCCATTAC-3' and 5'-AGCGTAATACGACTCACTATAGGAGAACCTGTTGATTCAACAG CACC-3' primers to generate a biotin-16-dUTP (Roche) labeled dsDNA probe of the 10366-10723 nucleotides of the 3'-UTR sequence. Briefly, 32 µg of total RNA mixed with loading dye was separated on a 1% agarose gel. The gel was then soaked in alkaline buffer (NaOH 0.01 N/ NaCl 3 M) for 20 min and equilibrated 5 min in transfer buffer. Transfer to a nylon membrane (Biodyne B) was conducted by downward transfer as detailed in the NorthernMax kit protocol. After UV cross-linking, the membrane was subjected to two cycles of pre-hybridization with ULTRAhyb-oligo buffer (Ambion) at 42 °C for 30 min 800 ng of dsDNA labeled probe diluted in 10 mM EDTA was denatured for 10 min at 95 °C, immediately mixed with ULTRAhyb-oligo buffer and incubated overnight at 42 °C on a rotating oven. Subsequently, the membrane was washed and blocked with 1% SDS Odyssey blocking buffer (TBS) (Li-cor) and stained at RT for 60 min with IRDYE 800cw streptavidin (Li-cor). The image was taken with Odyssey CLx imaging system (Li-Cor) and analyzed by Image Studio Lite (Li-cor) to quantify blots.

2.17. In silico analysis

The nucleotide sequences obtained from the sequencing were translated by Translated tool (https://web.expasy.org/translate/). The multiple alignments of the proteins were performed using T-COFFEE server (http://tcoffee.crg.cat/apps/tcoffee/do:expresso).

The RNA secondary structures of the 5'- (1–96 nt) and 3′- (10295–10444 nt) UTRs were determined using RNAalifold WebServer (http://rna.tbi.univie.ac.at/cgi-bin/RNAWebSuite/RNAalifold.cgi) and RNA structure 6.0.1 software. DENV 2 New Guinea (GenBank access number AF038403) was used as a reference strain. The analysis of defective viral genomes in next-generation sequencing data was performed with ViReMa, a Virus Recombination Mapper, as previously reported (Routh and Johnson, 2014).

2.18. Statistics

For the statistical analysis, the Graph Pad Prism software version 6.0 was used. The one-way ANOVA test with the Bonferroni post-hoc test for multiple comparisons and the Student's *t*-test was applied, depending on the number of conditions or groups that were analyzed. Data were expressed with the value of means and the standard deviations (SD), and statistical significance was considered as p-value ≤ 0.05.

2.19. Ethics statement

This study was conducted by the Official Mexican Standard Guidelines for Production, Care and Use of Laboratory Animals (NOM-062-ZOO-1999) and the protocol, number 048–02, was approved by the Animal Care and Use Committee (CICUAL) at CINVESTAV-IPN, Mexico.

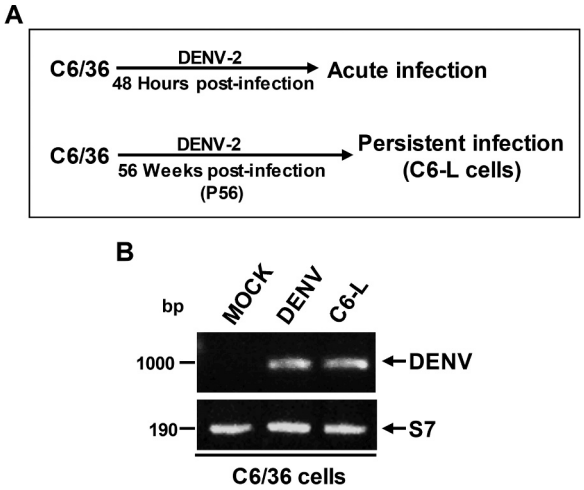

Fig. 1. DENV genome is detected in the C6-L cells. (A) Schematic representation of the persistent (56 weeks post-infection or passage 56) and acute viral infections (48 h post-infection) in C6/36 cells used in this study. (B) The amplification of the DENV NS4A-NS4B-NS5 region is shown as a 1,019-bp amplicon in DENV-infected C6/36 cells (DENV), and in C6/36 cells persistently infected with DENV (C6-L) but not in mock-infected cells (MOCK). The amplicons of the *Aedes aegypti* ribosomal S7 gene (190-bp amplicon) are present in all conditions (S7).

2.20. Nucleotide sequence accession numbers

The complete genomes of the DENV isolated from C6/36 cells infected by 48 h, 30 weeks (passage 30), and 56 weeks (passage 56) have been submitted to GenBank under the accession numbers MH613984, MH613985, and MH613986, respectively.

3. Results

3.1. Viral particles released from C6-L cells are not detected in the tests using mammalian cells

Since C6-L cells do not produce infectious viral particles for BHK-21 cells at 42 weeks post-infection (Juárez-Martínez et al., 2013) the first step was to determine if the C6-L cells release infectious viral particles into extracellular space. Thus, RT-PCR and plaque assays were performed using passage 56 of C6-L cells (56 weeks post-infection, P56) and compared to C6/36 cells infected for 48 h with DENV 2 as a model of acute infection (Fig. 1A).

DENV infection in the P56 was analyzed by RT-PCR using total RNA and specific primers to amplify the DENV NS4A-NS4B-NS5 region since this passage showed no cytopathic effect (CPE) or infectious viral particles for BHK-21 cells (Juárez-Martínez et al., 2013). The 1,019-bp amplicon was observed in the DENV-infected C6/36 cells and C6-L cells but not in mock-infected cells. Primers for the ribosomal S7 gene were used as an internal control, and its presence was confirmed in all samples (Fig. 1B).

To analyze the presence of infectious viral particles from C6-L cells, the viral yield from the supernatant (SN) of the P56 was determined by plaque assay in BHK-21 monolayers. As it can be observed, no lytic plaques were detected when the SN from C6-L cells was used, even when undiluted, in contrast with the SN of DENV-infected C6/36 cells (Fig. 2A and C). To determine if the defect in viral particle production was specific to DENV, the viral yield of the supernatant from C6-L cells

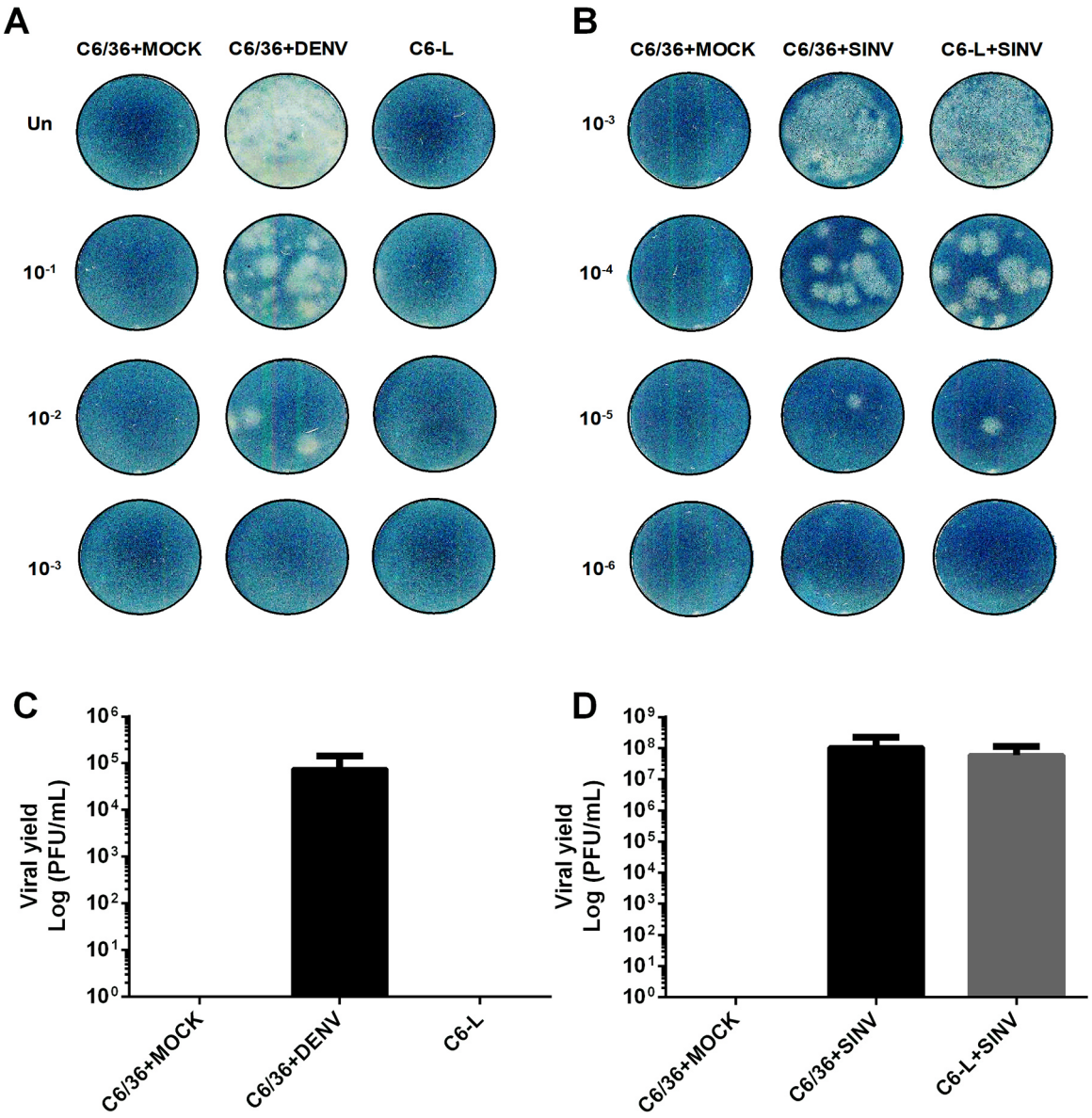

Fig. 2. The DENV particles from C6-L cells are not detected by plaque assay. (A and B) The viral yield of the supernatants from mock-infected C6/36 cells (C6/36 + MOCK), DENV-infected C6/36 cells (C6/36 + DENV), C6/36 cells persistently infected with DENV 2 (C6-L), SINV-infected C6/36 cells (C6/36 + SINV), and SINV-infected C6-L cells (C6-L + SINV) was determined by plaque assay in BHK-21 monolayers. The undiluted (Un), and the 10-fold dilution series are indicated on the left side of each multi-well plate. (C and D) The results were expressed in the log of PFU/mL from three independent assays.

infected with Sindbis virus (SINV), an alphavirus member of the *Togaviridae* family that can infect C6/36 cells, was determined. Interestingly, the C6-L cells were able to produce infectious SINV particles similarly to SINV-infected C6/36 cells (Fig. 2B and D), indicating that the impairment in generating infectious viral particles was specific for DENV 2 and that the C6-L cells were able to support a productive infection of a non-homologous virus. Additionally, to confirm the infective capacity of the viral particles from cells persistently infected with DENV, the SN from C6-L cells was inoculated intracerebrally into suckling Balb/c mice, and the number of surviving animals was monitored over a 15-day time to detect infectious viral particles. Only the mice inoculated with the SN from C6/36 cells infected with DENV for 48 h died 4–8 days post-inoculation, and all mice inoculated with the SN from C6-L cells survived (Fig. 3A), suggesting an absence of infectious viral particles for mammalian cells in the culture medium from C6/36 cells persistently infected with DENV 2. Since this apparent absence of DENV infectious particles for mammalian cells could be a consequence of a defect in the maturation or exit of the virions, intracellular and extracellular viral particles were recovered, and the viral yield was determined by plaque assay. Again, no lytic plaques were observed either in samples from the cellular fraction or the culture medium of the P56 from C6-L cells, in contrast with the supernatant of the acutely infected C6/36 cells (Fig. 3B and C) that caused greater amounts of plaque forming units than the intracellular fraction. These results suggest that although the DENV genome can be found in the C6-L cells, no infectious viral particles for mammalian cells are produced.

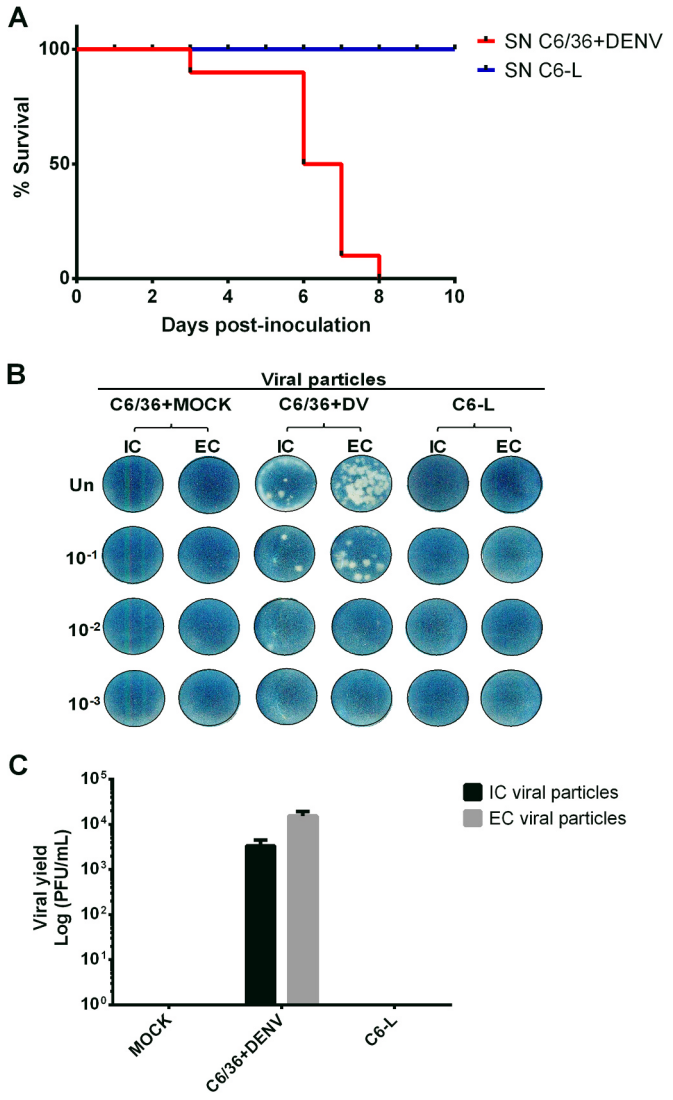

Fig. 3. The viral particles from C6-L cells do not infect mice and BHK-21 cells. (A) Suckling Balb/c mice were inoculated through the intracerebral route with five microliters of supernatant from DENV-infected C6/36 cells (SN C6/36 + DENV) or C6-L cells (SN C6-L). The lethality of mice infected (n = 10) was determined for 15 days. (B and C) The viral yield of the intracellular (IC) or extracellular (EC) virus from mock-infected C6/36 cells (C6/36 + MOCK), C6/36 cells persistently infected (C6-L) or acutely infected with DENV 2 (C6/36 + DV) was determined by plaque assay in BHK-21 monolayers. The undiluted (Un), and the 10-fold dilution series are indicated on the left side of each multiwell plate. (C) The results were expressed in the log of PFU/mL from three independent assays.

3.2. The C6-L cells display DENV-induced membrane structures and produce infectious viral particles for mosquito cells

The next step was to determine if the absence of infective viral particles in the supernatant and intracellular fraction of the C6-L cells could be related to a defect in the DENV replication and assembly sites. Therefore, ultrastructural analysis of the persistently infected cells was performed by transmission electron microscopy (TEM). DENV-infected C6/36 cells were used as a control of acute infection, they showed membrane invaginations of the endoplasmic reticulum (ER), such as double-membrane vesicles (Ve) (Junjhon et al., 2014; Reyes-Ruiz et al., 2018), and the presence of virus-like particles (Vi) (electron-dense small spheres corresponding to the morphology and size of the viral particles) were observed within distended reticulum membranes (Fig. 4A). Interestingly, the same complex sets of virus-induced subcellular structures in acutely infected C6/36 cells were observed in the

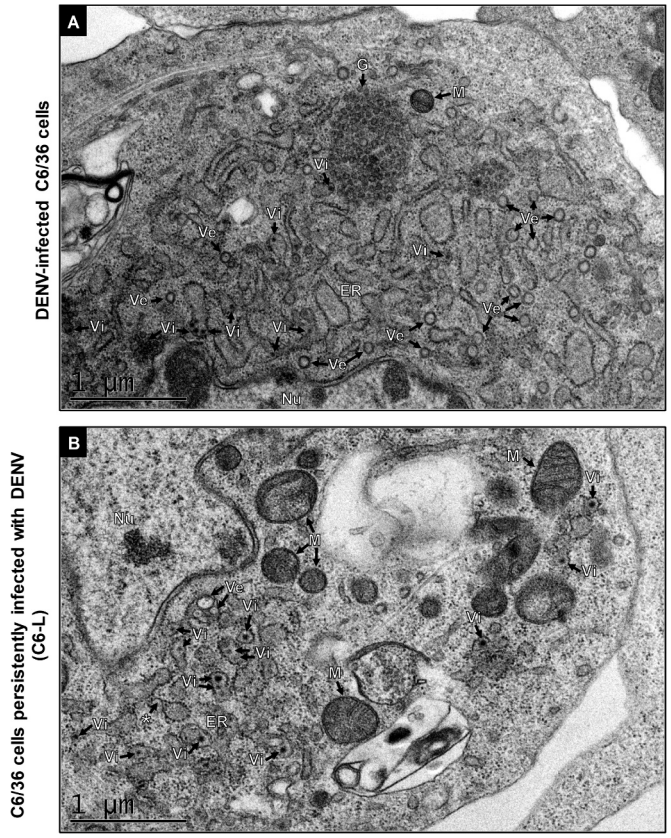

Fig. 4. The C6-L cells show intracellular membrane rearrangements induced by dengue virus. (A) C6/36 monolayers infected with DENV 2 at an MOI of 1 for 48 h or (B) C6-L monolayers were fixed and processed for transmission electron microscopy (TEM). Ve, double-membrane vesicles; Vi, virus-like particles; ER, endoplasmic reticulum; Nu, nucleus; M, mitochondria; G, Golgi apparatus; and (*), a putative event of viral budding into the ER.

C6-L cells (Fig. 4B). Moreover, virus-like particles (Vi) were observed in the distended reticulum membrane (Figs. 4B and 5A), between the cells and in the extracellular space (Fig. 5B). Additionally, several Ve contained irregular thread-like electron-dense material previously identified and described as the viral replication complexes (RC) (Junjhon et al., 2014) (Figs. 4B and 5A) were observed. Remarkably, the C6-L cells had structures that have been previously reported as membrane packets (Vp) (Junjhon et al., 2014) which enclosed of 3–10 Ve and contained ribosomes attached to their surfaces (Fig. 5A). These results indicated that viral morphogenesis and the release of viral particles are both taking place in the P56 from C6-L cells.

To confirm the association between the ER membrane rearrangements observed by TEM and the viral infection, immunoelectron microscopy (IEM) analysis using an antibody against the NS3 protein was performed. The anti-NS3 antibody showed specific labeling in ER sections close to the Vp and Ve structures in DENV-infected cells (Fig. 5C) and the C6-L cells (Fig. 5D). Thus, since NS3 viral protein has helicase activity that is required for RNA synthesis (Matusan et al., 2001), its localization suggests that the invaginations of the ER membrane observed in C6-L cells corresponded to the viral replication complexes (Junjhon et al., 2014; Welsch et al., 2009).

The TEM and IEM analysis strongly suggest that the P56 of C6-L cells have replication complexes and produce viral particles. Finally, to corroborate the presence of the viral particles and demonstrate its infectivity capacity, qRT-PCR and flow cytometry assays were performed in C6-L cells and C6/36 cells treated with the supernatant of the P56

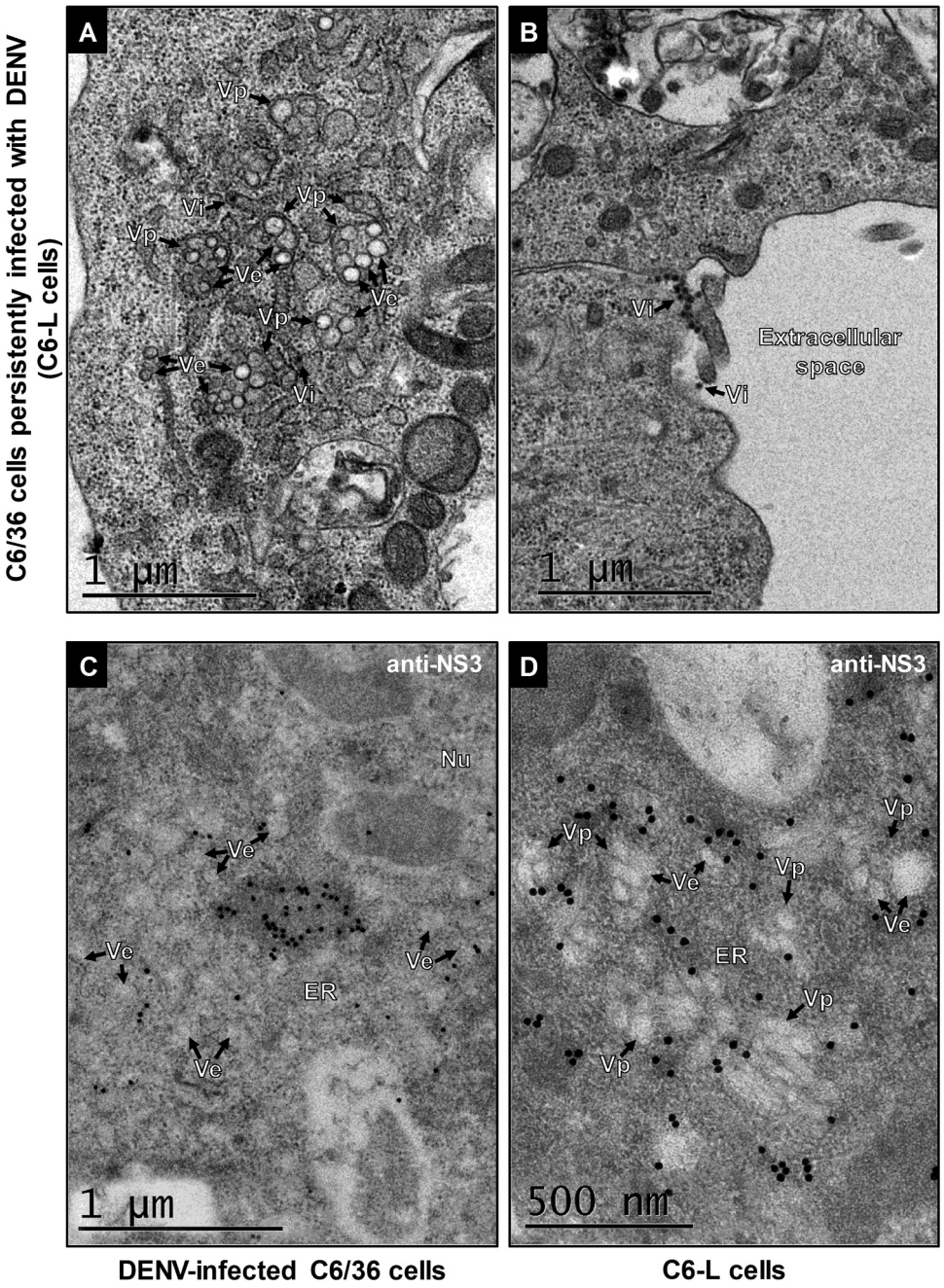

Fig. 5. The C6-L cells contain DENV replication and assembly sites. (A, B, and D) C6/36 monolayers persistently infected with DENV 2 (C6-L cells) or (C) C6/36 cells infected with DENV 2 at an MOI of 5 for 48 h were fixed and processed for TEM (A and B) and immunoelectron microscopy (IEM) (C and D) using an anti-NS3 antibody. The specific labeling signal to NS3 is shown as dark spots. Ve, double-membrane vesicles; Vi, virus-like particles; Vp, membrane packets; ER, endoplasmic reticulum; and Nu, nucleus.

from C6-L cells. Interestingly, in C6-L cells and their supernatant was found a high number of viral RNA copies in contrast with DENV-infected cells (Fig. 6A). Surprisingly, viral RNA copies were also detected in C6/36 cells treated with the SN from C6-L cells (Fig. 6A), suggesting

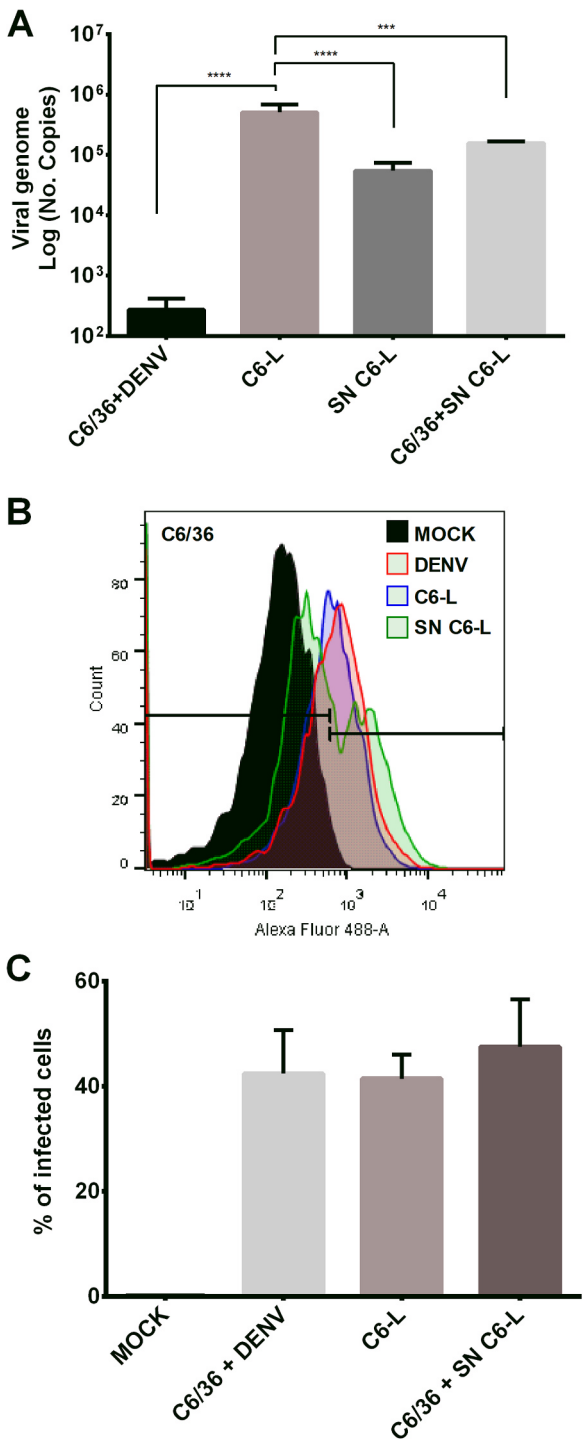

Fig. 6. The viral particles produced from C6-L cells can infect C6/36 cells. (A) The viral RNA levels of DENV-infected C6/36 cells (C6/36 + DENV), C6-L cells (C6-L), supernatant (SN) from C6-L cells (SN C6-L), and C6/36 cells treated with the SN from C6-L cells (C6/36 + SN C6-L) were determined by qRT-PCR. The log of the number of copies of RNA ± SD from three independent assays in duplicate is represented (***$p = < 0.001$, ****$p = < 0.0001$). (B and C) The percentage of cells infected of the conditions: mock-infected C6/36 cells, DENV-infected C6/36 cells, C6-L cells, and C6/36 cells treated with the SN from C6-L cells, was determined by flow cytometry using the anti-prM/E antibody.

that the viral particles released into the extracellular space by C6-L cells are infective to C6/36 mosquito cells. When the number of infected cells was evaluated by flow cytometry, approximately 40% of the C6-L cells and C6/36 cells treated with the SN from C6-L cells were positive for the anti-prM/E antibody (Fig. 6B and C). To confirm these results, TEM and IEM analysis were performed using an anti-NS3 antibody in the IEM. As shown in Fig. 7A, virus-like particles (Vi) were found in C6/36 cells treated with the SN from C6-L cells. These Vi were closely associated with the Vp, which contained ribosomes attached to their surfaces and enclosed 3–6 Ve. Also, the Vi were observed between cells (Fig. 7B), and the anti-NS3 antibody was able to recognize the protein associated with the virus-induced membrane rearrangements (Fig. 7C) confirming the presence of the viral replication complexes. These results demonstrate the presence of replication complexes in the P56 from C6-L cells and the production and release of infectious viral particles for mosquito cells.

3.3. Viral particles released from C6-L cells do not infect mammalian cells

Although the previous results strongly suggested that the C6-L cells were able to generate infectious viral particles in mosquito cells, they were not able to generate lytic plaques in BHK-21 cells. One possible explanation for this is that the viral particles produced from the C6-L cells were unable to infect mammalian cells. To evaluate this possibility, three different mammalian cell lines (BHK-21, Vero, and Huh-7 cells) were treated with the supernatant of the P56 from C6-L cells, and the viral infection was evaluated by confocal microscopy using an anti-prM/E antibody. Interestingly, the viral particles released from C6-L cells were unable to infect the BHK-21, Vero, and Huh-7 cells compared to the cells treated with the wild-type (WT) DENV 2 (Fig. 8A). However, the viral particles obtained from C6-L cells were able to infect C6/36 cells (Fig. 8B). In the same way, Aag2 cells were infected with supernatant from C6-L cells and analyzed by confocal microscopy. Interestingly, the Aag2 cells were permissive to infection by the viral particles released from C6-L cells (Fig. 8B). These results support the idea that the viral particles produced by C6-L cells are not able to infect mammalian cells.

In order to determine the specific step of the DENV replicative cycle restricted in mammalian cells; viral binding, viral entry, and replication assays were performed. Since Huh-7 cells have a human origin, we selected them to perform these experiments using viral particles from C6-L cells. First, the viral binding assay was performed by flow cytometry using an anti-DENV 2 antibody and demonstrated that the viral particles from C6-L cells were able to bind to the surface of Huh-7 cells in the same manner that the WT DENV (Fig. 9); supporting the idea that the viral particles released from C6-L cells can bind to the surface of mammalian cells. The next step was to evaluate the viral entry process. Since after DENV binding, the viral particle is internalized, and the capsid protein/genome complex is released into the cytoplasm, confocal microscopy, flow cytometry, and western blot analysis were performed using an anti-C antibody in Huh-7 cells treated with the viral particles of the P56 from C6-L cells for 1 h. As shown in Fig. 10A, the presence of the viral protein C was detected (in red) by confocal microscopy in the cytoplasm of the cells treated with the WT DENV and the viral particles from the C6-L cells. The ability of the viral particles released from C6-L to enter the Huh-7 cells was confirmed by flow cytometry (Fig. 10B and C) and western blot (Fig. 10D) where the C protein was also detected. Together, these results indicate that the viral particles from C6-L cells can bind and enter into the Huh-7 cells. Finally, to analyze the replicative ability of these viruses in Huh-7 cells, an RT-PCR assay was performed using primers for the viral capsid-coding region. An amplicon of 151 bp corresponding to C gene was detected in Huh-7 cells infected with the WT DENV 2, although interestingly, the amplicon was not detected when these cells were treated with the SN from C6-L cells (Fig. 11). All these results indicate that the viral particles produced during the persistent infection in C6/36 cells

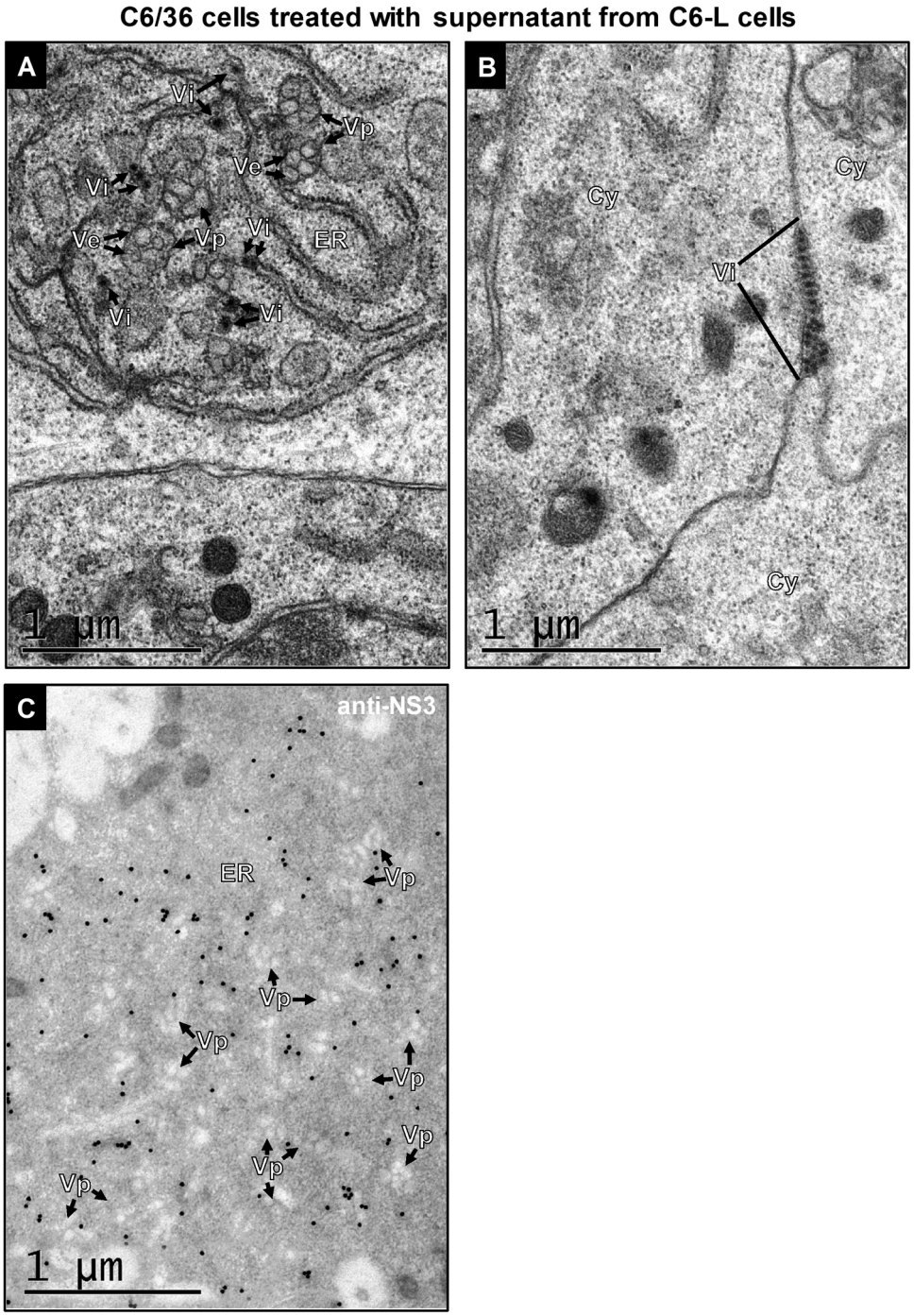

Fig. 7. The viral particles released from C6-L cells induce the rearrange endoplasmic reticulum membranes in C6/36 cells: formation of replication complexes. C6/36 monolayers were treated with the supernatant from C6-L cells for 48 h. Then, the cells were fixed and processed for TEM (A and B) and IEM (C) using an anti-NS3 protein antibody. The specific labeling signal to NS3 is shown as dark spots. Ve, double-membrane vesicles; Vi, virus-like particles; Vp, membrane packets; ER, endoplasmic reticulum; and Cy, cytoplasm.

underwent a modification that allowed them to infect the mosquito cells but not the mammalian cells. Thus, the restriction for the propagation of these viral particles in mammalian cells seems to occur at the replicative level.

3.4. Viral genome of the particles released from C6-L cells displays several mutations

To determine if the cell-type restriction of infection by viral particles from C6-L cells could be associated with changes in the viral genome, RNAseq of the viral particles released from passages 30 (P30) and 56 (P56) was performed. Additionally, the genome of viral particles released from DENV-infected C6/36 cells at 48 h was also isolated and sequenced. Variants in the genome sequences were readily identified by aligning the RNAseq data to the reference New Guinea C (NGC) strain of DENV 2 (NCBI accession number AF038403). Consensus genomes for each sample were thus generated revealing that the P56 from C6-L cells had 35 single nucleotide variants (SNVs) by comparison to DENV 2 genomes of particles released at 48 hpi (acute infection), of which 24 were non-synonymous amino acid-encoding SNVs (Table 1). These

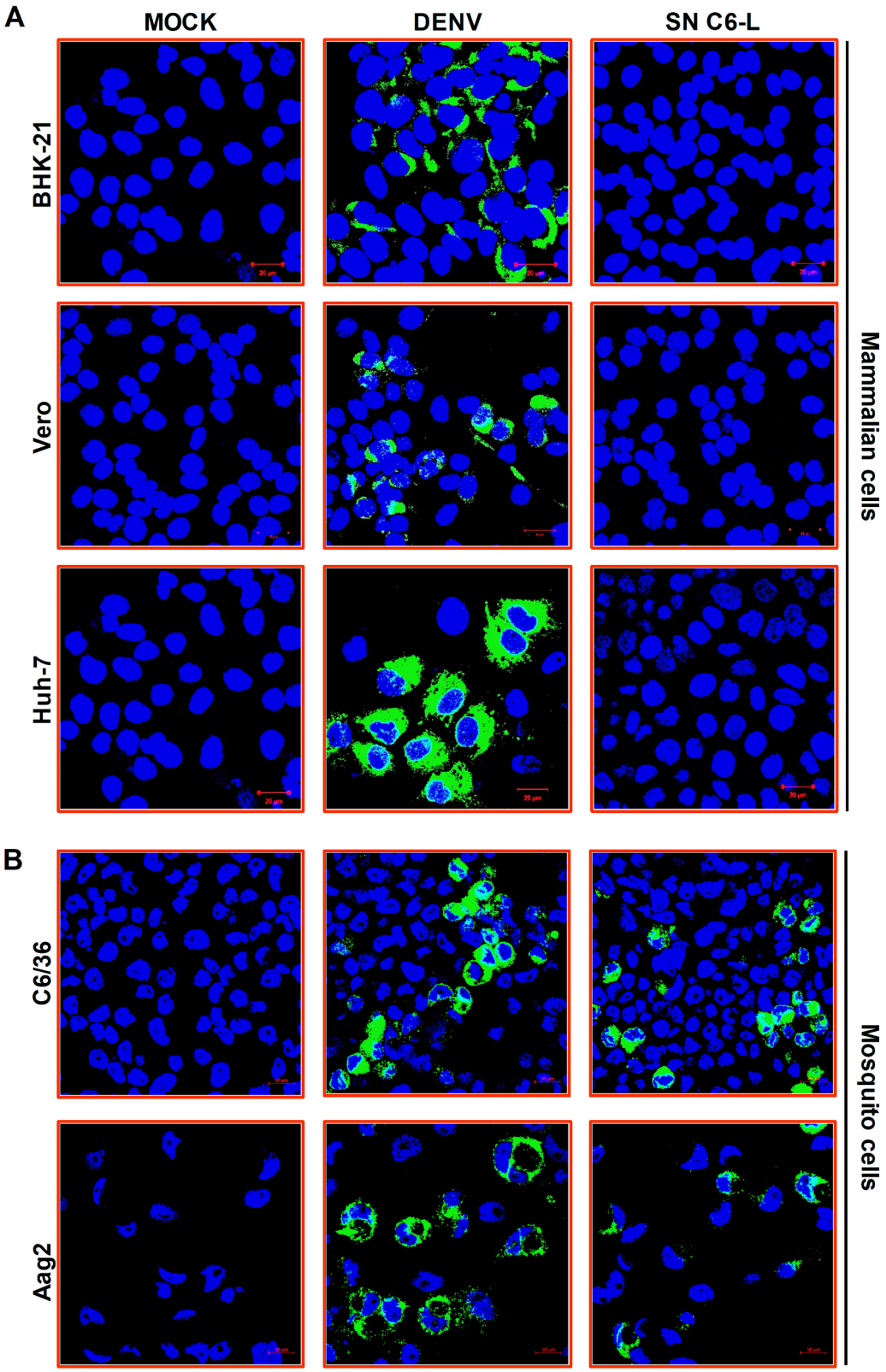

Fig. 8. The viral particles produced from the C6-L cells infect mosquito cells but not mammalian cells. (A) Mammalian (BHK-21, Vero, Huh-7 cells) and (B) mosquito cells (C6/36 and Aag2 cells) were mock-infected, infected with DENV, or treated with the supernatant from C6-L cells (SN C6-L) for 48 h. The viral infection was evaluated by confocal microscopy using the anti-prM/E antibody (green). The nuclei were stained with Hoechst (blue), and a representative image of each condition is shown.

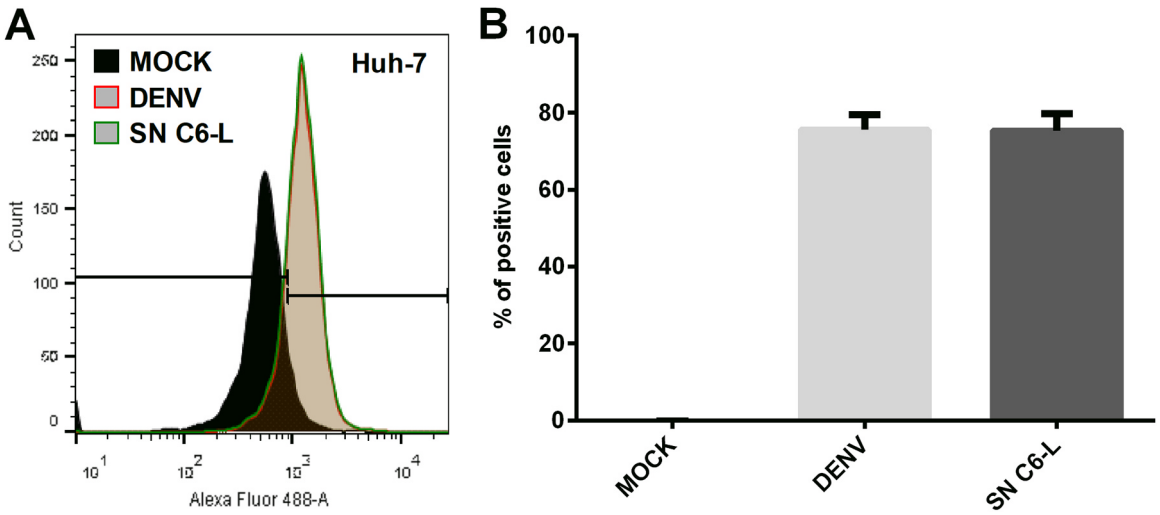

Fig. 9. The viral particles released from the C6-L cells can bind to Huh-7 cells surface. (A and B) Huh-7 cells were incubated for 30 min at 4 °C with DENV 2 (DENV), supernatant from C6-L cells (SN C6-L) or without virus (MOCK). The amount of virus attached to the surface of the cells was evaluated by flow cytometry using an anti-DENV 2 antibody.

yields had a Ka/Ks ratio of 1.5, indicating positive selection in the P56 strain at the protein level. Moreover, five mutations were only found in the P56: c.4719 A > T, c.7169 T > C, c.7486 A > G, c.7602 G > A, and c.9174 C > A. The first of these mutations were in NS3 (p. E66D), two are in the open reading frame (ORF) for the NS4B protein resulting in the change of Valine for Alanine (p. V115A), and Methionine for Valine (p. M221V). The other two mutations were in the NS5 protein coding region but did not result in amino acid changes. The remaining 30 mutations were found across the viral genome: one in 5′- and 3′-UTRs, one in prM, five in E, five in NS1, two in NS2B, four more in NS3, two in NS4A, three more in NS4B, and six additional in NS5 proteins. Also, some mutations changed hydrophobic amino acid to another hydrophobic amino acid. We next analyzed the effect that nucleotide substitutions might have on the DENV 5'- and 3'-UTRs of the viral particles produced by the P30 and P56 from C6-L cells.

3.5. The DENV 5'- and 3'-UTRs of the P30 and P56 undergoes conformational changes

Since the DENV 5'- and 3'-UTRs are essential for viral replication and translation (Alvarez et al., 2008; Filomatori et al., 2006; Friebe et al., 2011; Manzano et al., 2011; Villordo et al., 2015; Villordo and Gamarnik, 2013), the structural conformations of this region of the DENV P30 and P56 were evaluated and compared with the sequence of the WT and DENV of 48 hpi. To predict the RNA secondary structures of the 5' and 3′ UTRs the complete 5' UTR (1–96 nt) and the sequence of nucleotides corresponding to the variable region of the DENV 3'-UTR (10295–10444 nt) (Villordo et al., 2015) were used. The *in silico* analysis by RNAalifold showed that the mutation c.59 T > C located in the large stem-loop A (SLA) of the 5'-UTR causes a change in its structure, creating an additional loop in the stem 2 (S2) (Fig. 12). On the other hand, the predicted folds for the 3'-UTR of the P30 and P56 of DENV showed that the mutation c.10403 T > A located in the stem-loop II (SLII) produces an enlargement of their top loop where are found the nucleotides involved in the formation of pseudoknot II (PKII), in contrast to 3'-UTR of WT (Fig. 13). Interestingly, this conformational change was also observed in the top loop of the SLII of DENV obtained from 48 hpi (acutely infected C6/36 cells) where occurs a c.10403 T > C change.

Since it has been previously reported that mutations in the SLII are related to the generation of different populations of subgenomic flavivirus RNA (sfRNA) (Filomatori et al., 2017), a Northern-blot assay was performed using a biotinylated probe targeting the 3′-UTR and RNA from both acutely infected C6/36 cells and the P56 from C6-L cells. Interestingly, the P56 from C6-L cells produced almost 15 times more sfRNAs that the acutely infected C6/36 cells (Fig. 14A and B) suggesting that the mutation c.10403 T > A favored their production. Additionally, an additional band slightly smaller than the viral genomic RNA was detected only in C6-L cells (Fig. 14A). To confirm this observation, the nucleotide sequence of P56 was analyzed with ViReMa (Viral-Recombination-Mapper) which detects defective viral genomes in next-generation sequencing data (Routh and Johnson, 2014). The most common recombination event was a deletion event from nucleotide 8937 to nucleotide 10091. There were 122 reads that mapped over this event in the P56. Since the wild-type coverage in this region was 3500–8000 reads, this deletion would account for ~3% of the total genomes and correlates with the size of the additional band observed in Fig. 14A. This result is consistent with our previous findings (Juárez-Martínez et al., 2013).

All these results indicate that viral particles produced during the persistent infection display changes in viral replication fitness in a host-dependent manner that are associated with some mutations in the viral genome.

4. Discussion

The arboviruses can establish long-term infections in their vectors known as persistent infections (Blair, 2011; Goic and Saleh, 2012; Sánchez-Vargas et al., 2009). Vertical transmission in nature, where the viruses are transmitted from an infected female mosquito to her progeny is one mechanism that may allow DENV to remain in an environment during interepidemic periods (Apodaca-Medina et al., 2018; Edillo et al., 2015; Günther et al., 2007; Gutiérrez-Bugallo et al., 2017; Martins et al., 2012; Thenmozhi et al., 2007). Therefore, the persistence of the virus in the mosquito cells could have a potential impact on the DENV vertical transmission. Since these kinds of infections are difficult to study using mosquitoes, even under temperature controlled conditions where the insects can survive up to 38 days (Goindin et al., 2015), C6/36 *Aedes albopictus* mosquito cells have been used as a model to study persistent infections with DENV (Chen et al., 1994; Igarashi, 1979; Kanthong et al., 2008). In this sense, C6-L cells (Juárez-Martínez et al., 2013) have shown initially similar patterns in viral titer over time to those reported previously for DENV (Chen et al., 1994) and other arboviruses such as Bunyamwera (Elliott and Wilkie, 1986; Newton

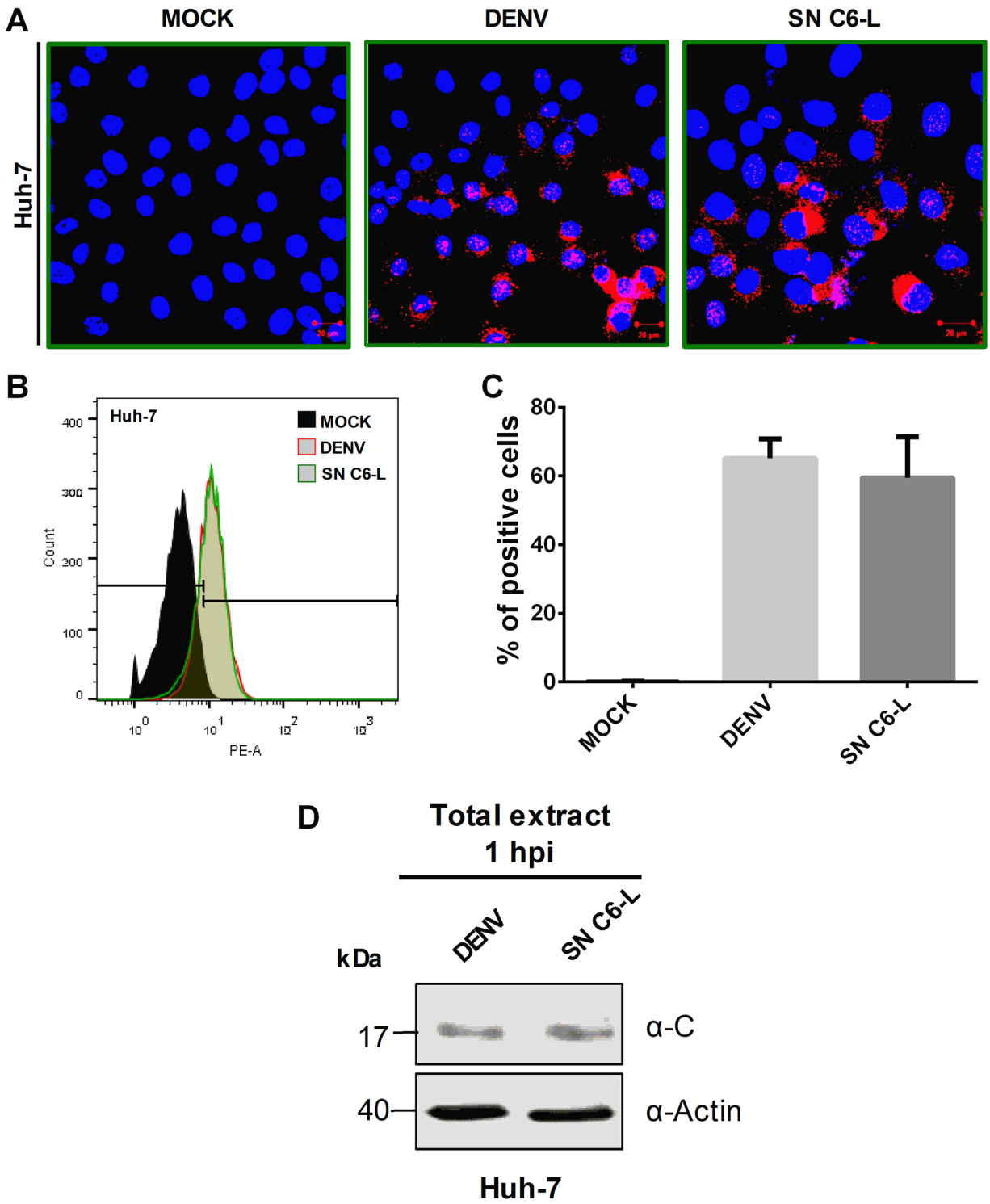

Fig. 10. The viral particles produced from C6-L cells enter to Huh-7 cells. Monolayers of Huh-7 cells were incubated for 1 h with DENV 2 (DENV), supernatant from C6-L cells (SN C6-L) or without virus (MOCK). The viral internalization was analyzed by confocal microscopy (A), flow cytometry (B and C), and Western blot (D) using an anti-C antibody. In the case of confocal microscopy, the viral C protein is observed in red, the nuclei were stained with Hoechst (blue), and a representative image of each condition is shown.

et al., 1981). Interestingly, at 42 weeks post-infection (passage 42), the viral particles were no longer detected by plaque assay in BHK-21 cells, which suggested clearance of the infection. However, the viral genome and viral proteins were detected, indicated that the C6-L cells were still infected by DENV (Juárez-Martínez et al., 2013), but probably impaired to generate infectious viral particles. Consequently, to investigate this possibility, the detection of viral particles and their infective capacity were analyzed in the present work. One initial approach was to infect C6-L cells with another virus and analyze the infectivity of the viral progeny in BHK-21 cells. SINV was able to infect C6/36 and C6-L cells similarly, indicated that the persistently infected cells with DENV were still able to support viral morphogenesis of an unrelated alphavirus. This result is consistent with C6/36 cells persistently infected with SINV that can be infected by an unrelated flavivirus (Karpf et al., 1997) or

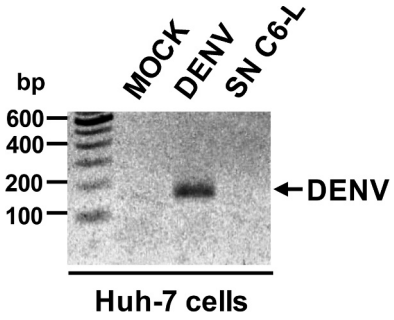

Fig. 11. Viral genome of the DENV particles from C6-L cells does not replicate in Huh-7 cells. Huh-7 monolayers were mock-infected (MOCK), DENV-infected (DENV), or treated with the supernatant from C6-L cells (SN C6-L) for 48 h. The detection of the viral genome was determined by RT-PCR using primers for the DENV C region (151-bp fragment).

Aedes albopictus cells persistently infected with Bunyamwera virus (Elliott and Wilkie, 1986; Newton et al., 1981). Also, neither intracellular nor extracellular DENV infectious particles could be detected which suggests that this defect was specific for DENV. On the other hand, ultrastructural changes associated with DENV infection were observed in C6-L cells indicating that viral replication remains active. Moreover, the formation of replication complexes and viral particles in the C6-L cells and C6/36 cells treated with the supernatant from C6-L cells suggested that the viral morphogenesis was taking place in C6-L cells and that the virions produced by these cells can infect mosquito cells. These results are consistent with previous reports in *Aedes albopictus* cells persistently infected with DENV 2 (Kanthong et al., 2008) and SINV where the extracellular viruses play an essential role in maintaining persistent infection (Riedel and Brown, 1977).

One of the most interesting observations here was the inability of the viral particles released by C6-L cells to infect mammalian cells while still infecting mosquito cells. This impairment seems to occur at some point during the viral cycle after viral binding and entry since the viral particles from the C6-L cells supernatant were able to bind to the surfaces of the Huh-7 cells and enter similarly to the wild-type DENV. Also, the absence of the viral genome in Huh-7 cells infected with the viral particles from C6-L cells suggested a restriction of the viral replication in a host-dependent manner. Similar behavior has been observed in DENV 2 with mutations in one transmembrane domain of E protein (458LIGVII463). Deletions in this region allow replication in C6/36 cells but restrict it in Vero cells, and they did not revert to wild type phenotype after several passages in cell culture (Smith et al., 2011). However, we did not detect any mutations in this region in our study suggesting that the changes in viral fitness were not associated with the transmembrane domain of E protein.

It has been described that one of the consequences of the successive passages of a virus is the production of defective interfering (DI) particles along with the wild-type virus. These DI particles have deletions or point mutations in their genomes that confers them the incapacity to be infectious by themselves and always require the complementation of the parental virus (Huang and Baltimore, 1970). The DI particles are replicated preferentially inhibiting the replication of the parental virus (Rezelj et al., 2018) and have been reported during the infection with

Table 1
Consensus changes in the DENV 2 genome of viral particles produced by infected C6/36 cells.

	Nucleotide position	Viral genome				Amino acid changes	Coding region
		NGC strain	DENV2	Passage 30	Passage 56		
1	59	T	T	C	C	NONE	5′ UTR
2	601	T	C	T	T	L55F	prM
3	1149	T	A	T	T	D71E	E
4	1270	G	A	G	G	S112G	
5	1307	A	T	A	A	I124N	
6	1541	A	A	G	G	E202G	
7	2140	A	T	A	A	I402F	
8	2626	A	A	C	C	K69Q	NS1
9	2735	A	G	A	A	R105Q	
10	2941	A	G	A	A	E174K	
11	3103	T	T	C	C	S228P	
12	3130	T	C	T	T	NONE	
13	4169	T	T	C	C	M13T	NS2B
14	4472	T	T	C	C	I114T	
15	4719	A	A	A	T	E66D	NS3
16	5027	A	A	G	G	E169G	
17	5846	T	C	T	T	I442T	
18	5859	T	T	C	C	NONE	
19	6039	T	C	T	T	NONE	
20	6481	G	G	C	C	A36P	NS4A
21	6747	A	A	C	C	E124D	
22	6981	G	A	G	G	NONE	NS4B
23	7159	T	T	C	C	F112L	
24	7169	T	T	T	C	V115A	
25	7486	A	A	A	G	M221V	
26	7538	C	C	T	T	S238F	
27	7602	G	G	G	A	NONE	NS5
28	7801	G	G	C	C	V78L	
29	7866	A	A	G	G	NONE	
30	8238	T	T	C	C	NONE	
31	9174	C	C	C	A	NONE	
32	9357	A	G	A	A	NONE	
33	9715	T	T	G	G	L716V	
34	9970	C	C	A	A	H801N	
35	10403	T	C	A	A	NONE	3′ UTR

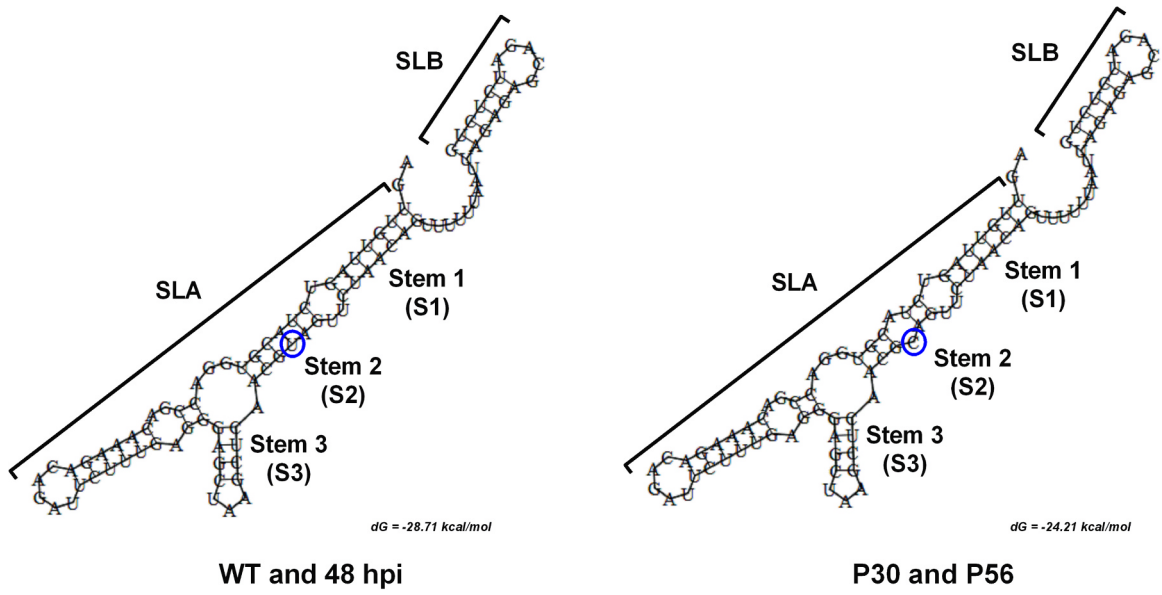

Fig. 12. The 5'-untranslated region (UTR) of the viral genome of the DENV particles produced from C6-L cells undergoes a conformational change. The models of the 5′-UTR showing the large stem-loop A (SLA) and short stem-loop B (SLB) for WT DENV (WT), DENV from C6/36 cells infected by 48 h (48 hpi), and DENV of the passages 30 and 56 from C6-L cells (P30 and P56) were performed with the RNAalifold web server. The mutation c.59 T > C of the P30 and P56 located in the stem 2 of SLA is shown with a blue circle.

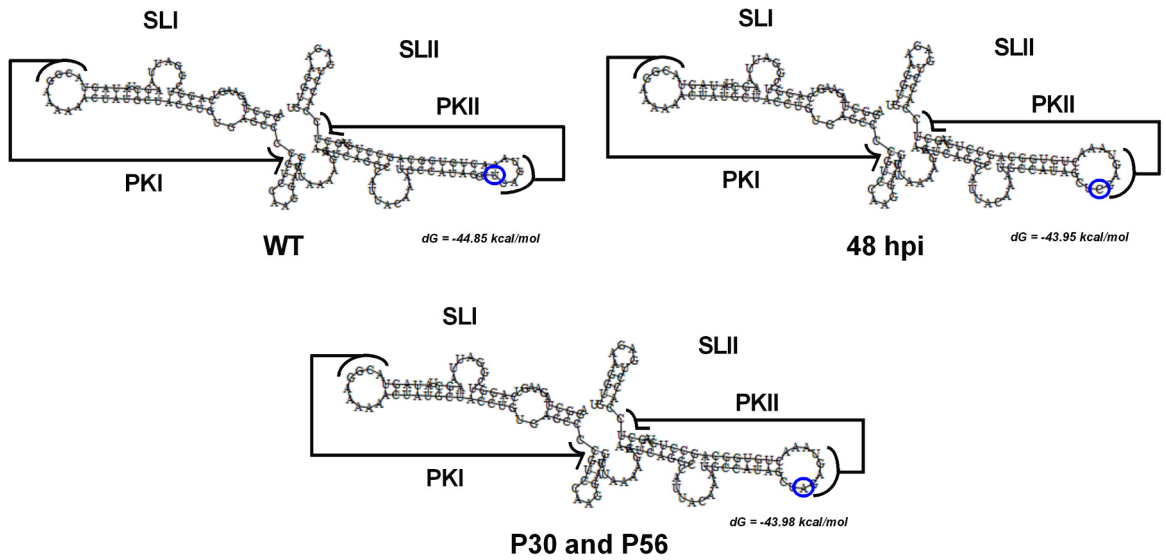

Fig. 13. The 3'-untranslated region (UTR) of the viral genome of the DENV particles from C6-L cells undergoes a conformational change. The models of stem-loop I (SLI) and stem-loop II (SLII) in the variable region of the DENV 3'-UTR were performed with the RNAalifold web server. The mutations c.10403 T > C of DENV from C6/36 cells infected by 48 h (48 hpi), and c.10403 T > A of the passages 30 and 56 of C6-L cells located in the SLII are shown with a blue circle. Also, the pseudoknots I and II (PKI and PKII) are indicated as has been reported by Villordo et al. (2015).

several flaviviruses (Aaskov et al., 2006; Li et al., 2011; Randolph and Hardy, 1988; Tsai et al., 2007; Yoon et al., 2006). Recently, the defective viral genomes associated with DI particles have been directly implicated in the maintenance of persistent infection in insect cells (Poirier et al., 2018). On the other hand, the oscillation in viral titers observed in C6-L cells during the first 42 weeks of infection (Juárez-Martínez et al., 2013) has been reported previously in C6/36 cells persistently infected with DENV (Chen et al., 1994; Igarashi, 1979) and in *Aedes albopictus* cells persistently infected with Bunyamwera virus (Elliott and Wilkie, 1986; Newton et al., 1981). This behavior has been associated with the presence of DI particles because they can compete with the wild-type virus during replication (Rezelj et al., 2018).

Additionally, the inability of the supernatant from C6-L cells to cause death in newborn mice intracerebrally inoculated has been observed previously (Igarashi, 1979; Newton et al., 1981). This phenomenon could be associated with the capacity of DI particles to interfere with the replication of the wild-type virus or to induce the antiviral immune response as has been reported for the respiratory syncytial virus (Sun et al., 2015). Finally, we detected a potent inhibition of the infection of viral particles released by C6-L cells that seems to be at the replicative level. Altogether, these results suggest that DI particles might be involved in this inhibition. In fact, defective viral genomes have been detected in C6-L cells previously (Juárez-Martínez et al., 2013) and we could corroborate its presence in the present work by northern blot assay and RNAseq, were we found a deletion event about 1153 nucleotides long from nucleotide 8937 to nucleotide 10091 in the sequence of P56.

Moreover, in this work, we identify some mutations previously

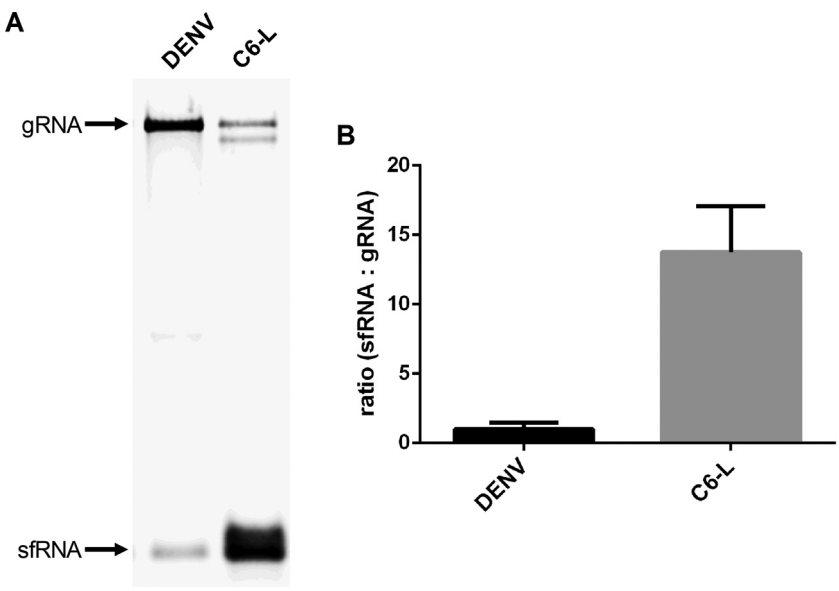

Fig. 14. The C6-L cells produce higher levels of sfRNA that the acutely infected cells. (A) Northern blot assay using a biotinylated probe targeting 3′ UTR of DENV and RNA from C6/36 cells infected with DENV for 48 h (DENV) or passage 56 of C6-L cells (C6-L). The viral genomic (gRNA) and the subgenomic flavivirus (sfRNA) RNAs are indicated by arrows. (B) Ratio of sfRNA: gRNA in C6/36 cells acutely and persistently infected. The statistic was performed using *t*-test.

detected in viral genomes present in the C6-L cells (Juárez-Martínez et al., 2013). For example, the mutation c.1541 A > G (p. E202G) in the domain II of the E protein coding region was also observed in the genome of the viral particles from C6-L cells after 60 weeks of persistent infection (P60) (Modis et al., 2003). Of note, a mutation in this position (p. K202R) has been previously observed in serially passaged DENV 3 in Vero cells and has been associated with changes in the fusion pH threshold (Lee et al., 1997). The E protein is responsible for viral binding and entry into the host cell, but since the viral particles produced from C6-L cells are still able to bind and enter to mammal cells, the relevance of this mutation is unclear. In the case of the NS5 protein, the amino acid changes p. V78L and p. L716V were detected in the P56 and also in the defective viral genomes in P60 (Juárez-Martínez et al., 2013). Although both amino acids are hydrophobic, their impact in the function of the protein needs to be addressed.

Even though the DI particles from C6-L cells might be participating in the inhibition of viral replication in mammal cells, this was not observed in mosquito cells. On the other hand, the deletion detected by RNAseq only account for ~3% of the total genomes which correlates with the northern blot assay performed here and previous data (Juárez-Martínez et al., 2013). Therefore, the number of defective viral genomes seems to be much less than the number of wild-type viral genomes and too low to inhibit viral replication, as has been observed in Huh-7 cells; suggesting that other factors might be involved in the change of viral fitness.

On the other hand, several studies have shown that serial passages of arbovirus in the same vector modify viral fitness in the vertebrate host. For example, 20 serial passages of West Nile virus (WNV) in *Culex* mosquitoes results in a decrease of the replicative fitness in chicks (Deardorff et al., 2011) and causes a reduction in the sizes of viral foci in Vero cells (Ciota et al., 2008). SLEV and WNV serially passaged in C6/36 cells exhibit slight decreases in the replicative fitness in the DF-1 cell line (Ciota et al., 2007). Similarly, 10 serial passages of two different strains of DENV 2 (sylvatic and endemic strain) in C6/36 cells results in viruses with reduced replicative fitness to Huh-7 cells (Vasilakis et al., 2009), and 9 serial passages of Murray Valley encephalitis virus (MVE) in Vero cells reduces growth rates in C6/36 cells and mice neuroblastoma cells and neurovirulence in mice (McMinn et al., 1995). These changes in replicative fitness have been associated with some mutations in the viral genome, that include the 3′-UTR (Ciota et al., 2009, 2008, 2007; Jerzak et al., 2007; McMinn et al., 1995; Vasilakis et al., 2009; Villordo et al., 2015). In this study, thirty-five mutations were detected in the DENV genome from C6/36 cells persistently infected with DENV 2. Some of these mutations might have an essential repercussion in viral replication. For example, the mutation c.9970 C > A caused a change of a positively charged amino acid to an uncharged polar amino acid (p. H801N) in the NS5, but this change is not predicted/expected to modify the structure of the viral protein (data not shown). Nevertheless, this amino acid change is found in the priming loop region of the DENV RdRp which plays an essential role in the control of conformational changes during the RdRp activity substantial to the replication (Yap et al., 2007). Thus, the mutation c.9970 G > A (p. H801N) may be crucial to the activity of the NS5.

Furthermore, two other mutations with possible important implications in viral replication were located in both UTRs of the viral genome. The DENV 2 particles produced by C6-L cells displayed a mutation (c.59 T > C) that results in the modification of the SLA structure. This structure is essential for the recruitment of the NS5 protein during RNA replication, and mutations in the bottom and the top loop of this structure abolish viral RNA synthesis (Filomatori et al., 2006). Although the c.59 T > C mutation present in the viral genome of persistently infected cells is not located in these crucial points, the modification of the structure might cause changes in the efficiency of the interaction of the NS5 protein with the SLA element in the context of the host cell. This hypothesis will require further investigation.

Additionally, one mutation was detected in the SLII of 3′-UTR of the viral genome of the particles produced by DENV-persistently infected C6/36. Previous reports have shown that after several passages of DENV 2 in C6/36 cells many mutations in the SLII of the 3′-UTR variable region are present and they correlate with a reduction in the capacity of these viral particles to infect BHK-21 cells (Villordo et al., 2015). However, the mutation detected in SLII of P30 and P56 was also found in the DENV of 48 hpi, thus, this structural change in the 3 ´UTR could be not related to DENV replication fitness in mammalian cells. Nevertheless, the mutations in the SLII are directly related to the generation of different populations of subgenomic flavivirus RNA (sfRNA) (Filomatori et al., 2017). The sfRNA are implicated in the regulation of several viral functions such as translation and replication, and cellular processes such as suppression of the RNAi response, and subversion of type I interferon signaling (Clarke et al., 2015; Roby et al., 2014). In this work, the C6-L cells showed an increased synthesis of sfRNA compared with acutely infected C6/36 cells. This observation is consistent with the ability of the viral particles released from C6-L cells to infect mosquito cells and that they might be able to evade the IFN-I response and infect mammal cells.

Interestingly, viral particles produced by the C6-L cells were unable

to infect either mammal cells or suckling Balb/c mice. Moreover, these particles were incapable of infect Vero cells as reported previously (Kanthong et al., 2008). Since the Vero cells are defective in the IFN-I response (Desmyter et al., 1968; Emeny and Morgan, 1979; Osada et al., 2014), additional factors other than the sfRNAs may be responsible for the interruption in viral replication of the mosquito-adapted viruses.

Remarkably, only five mutations were present in the P56 (c.4719 A > T, c.7169 T > C, c.7486 A > G, c.7602 G > A, and c.9174 C > A). These mutations result in amino acid changes in NS3 and NS4B proteins with probable repercussions in the viral phenotype since that viral particles from P56 only can replicate in mosquito cells but not in mammalian cells. The mutation found in the NS3 protein (c.4719 A > T; p. E66D) results in a synonymous amino acid change. Therefore, the repercussion of this mutation requires further investigation. However, recently, it has been demonstrated that the amino acid changes in the NS4B have a strong influence on viral fitness (Bui et al., 2018; Fujiki et al., 2018). Particularly, the mutation c.7169 T > C; p. V115A is located in the transmembrane domain 3 of NS4B (Li et al., 2015, 2016; Miller et al., 2006) which has been associated with an anti-IFN response (Bui et al., 2018; Muñoz-Jordán et al., 2005). Also, the amino acids 84–146 of NS4B are necessary for the NS4A-NS4B interaction involved in the viral replication (Zou et al., 2015). In this context, this mutation could result in an inability of viral particles released by C6-L cells to replicate and evade the antiviral response in Huh-7 cells.

Taken together, our results indicate that a viral adaptation occurs during the persistent infection process generating viral particles that are unable to successfully replicate in vertebrate cells, thus losing their ability to replicative in multiple hosts, a situation that resembles the dynamics of flaviviruses that only infect arthropods. This change in viral fitness is associated with several factors that include the presence of DI particles and several mutations in the viral genome, mainly in the genes encoding the NS4B and NS5 proteins and in both UTR regions, which are retained through the persistent infection.

Acknowledgments

We thank Mariana Salas-Benito for the maintenance of cell lines and mice, and Anel E. Lagunes-Guillén, Matilde García-Espitia, Fernando Medina, and Jaime Zarco for their technical assistance. We would like to thank Dr. Juan E. Ludert from CINVESTAV (Mexico) for their contributions to manuscript reviewing. This project was supported by Secretaría de Investigación y Posgrado (SIP 20151372) of Instituto Politécnico Nacional, Consejo Nacional de Ciencia y Tecnología (CONACYT, Mexico) Grant 220824, and Fundación Miguel Alemán. Drs. Salas-Benito and De Nova-Ocampo have fellowships from Estímulo al Desempeño de los Investigadores (EDI) and Comisión de Operación y Fomento a las Actividades Académicas (COFAA) from Instituto Politécnico Nacional. José Manuel Reyes-Ruiz, Juan Fidel Osuna-Ramos, and Juan Pablo Castillo-Munguía received scholarships from CONACYT.

References

Aaskov, J., Buzacott, K., Thu, H.M., Lowry, K., Holmes, E.C., 2006. Long-term transmission of defective RNA viruses in humans and Aedes Mosquitoes. Science 311, 236–238. https://doi.org/10.1126/science.1115030.

Alvarez, D.E., Filomatori, C.V., Gamarnik, A.V., 2008. Functional analysis of dengue virus cyclization sequences located at the 5′ and 3′UTRs. Virology 375, 223–235. https://doi.org/10.1016/j.virol.2008.01.014.

Apodaca-Medina, A.I., Torres-Avendaño, J.I., Rendón-Maldonado, J.G., Torres-Montoya, E.H., Flores-López, B.A., Del Angel, R.M., Velarde-Félix, J.S., Salomón-Soto, V.M., Castillo-Ureta, H., 2018. First evidence of vertical infection of dengue virus 2 in Aedes aegypti mosquitoes from Sinaloa, Mexico. Vector Borne Zoonotic Dis. 18, 231–233. https://doi.org/10.1089/vbz.2017.2202.

Bhatt, S., Gething, P.W., Brady, O.J., Messina, J.P., Farlow, A.W., Moyes, C.L., Drake, J.M., Brownstein, J.S., Hoen, A.G., Sankoh, O., Myers, M.F., George, D.B., Jaenisch, T., Wint, G.R.W., Simmons, C.P., Scott, T.W., Farrar, J.J., Hay, S.I., 2013. The global distribution and burden of dengue. Nature 496, 504–507. https://doi.org/10.1038/nature12060.

Blair, C.D., 2011. Mosquito RNAi is the major innate immune pathway controlling arbovirus infection and transmission. Future Microbiol. 6, 265–277. https://doi.org/10.2217/fmb.11.11.

Blair, C.D., Adelman, Z.N., Olson, K.E., 2000. Molecular strategies for interrupting arthropod-borne virus transmission by mosquitoes. Clin. Microbiol. Rev. 13, 651–661.

Bui, T.T., Moi, M.L., Nabeshima, T., Takemura, T., Nguyen, T.T., Nguyen, L.N., Pham, H.T.T., Nguyen, T.T.T., Manh, D.H., Dumre, S.P., Mizukami, S., Hirayama, K., Tajima, S., Le, M.T.Q., Aoyagi, K., Hasebe, F., Morita, K., 2018. A single amino acid substitution in the NS4B protein of Dengue virus confers enhanced virus growth and fitness in human cells in vitro through IFN-dependent host response. J. Gen. Virol. 99, 1044–1057. https://doi.org/10.1099/jgv.0.001092.

Chen, W.J., Chen, S.L., Fang, A.H., 1994. Phenotypic characteristics of dengue 2 virus persistently infected in a C6/36 clone of Aedes albopictus cells. Intervirology 37, 25–30.

Ciota, A.T., Jia, Y., Payne, A.F., Jerzak, G., Davis, L.J., S.Young, D., Ehrbar, D., Kramer, L.D., 2009. Experimental passage of St. Louis Encephalitis virus in vivo in mosquitoes and chickens reveals evolutionarily significant virus characteristics. PLoS One 4, e7876. https://doi.org/10.1371/journal.pone.0007876.

Ciota, A.T., Lovelace, A.O., Jia, Y., Davis, L.J., Young, D.S., Kramer, L.D., 2008. Characterization of mosquito-adapted West Nile virus. J. Gen. Virol. 89, 1633–1642. https://doi.org/10.1099/vir.0.2008/000893-0.

Ciota, A.T., Lovelace, A.O., Ngo, K.A., Le, A.N., Maffei, J.G., Franke, M.A., Payne, A.F., Jones, S.A., Kauffman, E.B., Kramer, L.D., 2007. Cell-specific adaptation of two flaviviruses following serial passage in mosquito cell culture. Virology 357, 165–174. https://doi.org/10.1016/j.virol.2006.08.005.

Clarke, B.D., Roby, J.A., Slonchak, A., Khromykh, A.A., 2015. Functional non-coding RNAs derived from the flavivirus 3′ untranslated region. Virus Res. 206, 53–61. https://doi.org/10.1016/j.virusres.2015.01.026.

Deardorff, E.R., Fitzpatrick, K.A., Jerzak, G.V.S., Shi, P.-Y., Kramer, L.D., Ebel, G.D., 2011. West Nile Virus experimental evolution in vivo and the trade-off hypothesis. PLoS Pathog. 7, e1002335. https://doi.org/10.1371/journal.ppat.1002335.

Desmyter, J., Melnick, J.L., Rawls, W.E., 1968. Defectiveness of interferon production and of Rubella virus interference in a line of African green monkey kidney cells (Vero). J. Virol. 2, 955–961.

Díaz, A., Kourí, G., Guzmán, M.G., Lobaina, L., Bravo, J., Ruiz, A., Ramos, A., Martínez, R., 1988. Description of the clinical picture of dengue hemorrhagic fever/dengue shock syndrome (DHF/DSS) in adults. Bull. Pan Am. Health Organ 22, 133–144.

Dittmar, D., Castro, A., Haines, H., 1982. Demonstration of interference between dengue virus types in cultured mosquito cells using monoclonal antibody probes. J. Gen. Virol. 59, 273–282. https://doi.org/10.1099/0022-1317-59-2-273.

Edillo, F.E., Sarcos, J.R., Sayson, S.L., 2015. Natural vertical transmission of dengue viruses in Aedes aegypti in selected sites in Cebu City, Philippines. J. Vector Ecol. 40, 282–291. https://doi.org/10.1111/jvec.12166.

Elliott, R.M., Wilkie, M.L., 1986. Persistent infection of Aedes albopictus C6/36 cells by Bunyamwera virus. Virology 150, 21–32. https://doi.org/10.1016/0042-6822(86)90262-X.

Emeny, J.M., Morgan, M.J., 1979. Regulation of the interferon system: evidence that Vero cells have a genetic defect in interferon production. J. Gen. Virol. 43, 247–252. https://doi.org/10.1099/0022-1317-43-1-247.

Filomatori, C.V., Carballeda, J.M., Villordo, S.M., Aguirre, S., Pallarés, H.M., Maestre, A.M., Sánchez-Vargas, I., Blair, C.D., Fabri, C., Morales, M.A., Fernandez-Sesma, A., Gamarnik, A.V., 2017. Dengue virus genomic variation associated with mosquito adaptation defines the pattern of viral non-coding RNAs and fitness in human cells. PLoS Pathog. 13, e1006265. https://doi.org/10.1371/journal.ppat.1006265.

Filomatori, C.V., Lodeiro, M.F., Alvarez, D.E., Samsa, M.M., Pietrasanta, L., Gamarnik, A.V., 2006. A 5′ RNA element promotes dengue virus RNA synthesis on a circular genome. Genes Dev. 20, 2238–2249. https://doi.org/10.1101/gad.1444206.

Focks, D.A., Haile, D.G., Daniels, E., Mount, G.A., 1993. Dynamic life table model for Aedes aegypti (diptera: Culicidae): simulation results and validation. J. Med. Entomol. 30, 1018–1028.

Friebe, P., Shi, P.-Y., Harris, E., 2011. The 5′ and 3′ downstream AUG region elements are required for mosquito-borne flavivirus RNA replication. J. Virol. 85, 1900–1905. https://doi.org/10.1128/JVI.02037-10.

Fujiki, J., Nobori, H., Sato, A., Sasaki, M., Carr, M., Hall, W.W., Orba, Y., Sawa, H., 2018. Single amino acid mutation in dengue virus NS4B protein has opposing effects on viral proliferation in mammalian and mosquito cells. Jpn. J. Infect. Dis. https://doi.org/10.7883/yoken.JJID.2018.107.

Gebhard, L.G., Filomatori, C.V., Gamarnik, A.V., 2011. Functional RNA elements in the dengue virus genome. Viruses 3, 1739–1756. https://doi.org/10.3390/v3091739.

Goic, B., Saleh, M.-C., 2012. Living with the enemy: viral persistent infections from a friendly viewpoint. Curr. Opin. Microbiol. 15, 531–537. https://doi.org/10.1016/j.mib.2012.06.002.

Goindin, D., Delannay, C., Ramdini, C., Gustave, J., Fouque, F., 2015. Parity and longevity of Aedes aegypti according to temperatures in controlled conditions and consequences on Dengue transmission risks. PLoS One 10. https://doi.org/10.1371/journal.pone.0135489.

Gould, E., Clegg, J., 1991. Growth, titration and purification of alphaviruses and flaviviruses. In: Mahy, B.W.J. (Ed.), Virology: A Practical Approach. IRL Press, Oxford, pp. 43–78.

Günther, J., Martínez-Muñoz, J.P., Pérez-Ishiwara, D.G., Salas-Benito, J., 2007. Evidence of vertical transmission of Dengue virus in two endemic localities in the state of Oaxaca, Mexico. INT 50, 347–352. https://doi.org/10.1159/000107272.

Gutiérrez-Bugallo, G., Rodriguez-Roche, R., Díaz, G., Vázquez, A.A., Alvarez, M., Rodríguez, M., Bisset, J.A., Guzman, M.G., 2017. First record of natural vertical transmission of dengue virus in Aedes aegypti from Cuba. Acta Trop. 174, 146–148.

https://doi.org/10.1016/j.actatropica.2017.07.012.
Hadinegoro, S.R.S., 2012. The revised who dengue case classification: does the system need to be modified? Paediatr. Int Child Health 32 (Suppl 1), 33–38. https://doi.org/10.1179/2046904712Z.00000000052.
Halstead, S.B., 2008. Dengue virus-mosquito interactions. Annu. Rev. Entomol. 53, 273–291. https://doi.org/10.1146/annurev.ento.53.103106.093326.
Huang, A.S., Baltimore, D., 1970. Defective Viral Particles and Viral Disease Processes. Nature 226, 325–327. https://doi.org/10.1038/226325a0.
Igarashi, A., 1979. Characteristics of Aedes albopictus cells persistently infected with dengue viruses. Nature 280, 690–691. https://doi.org/10.1038/280690a0.
Igarashi, A., 1978. Isolation of a Singh's Aedes albopictus cell clone sensitive to Dengue and Chikungunya viruses. J. Gen. Virol. 40, 531–544. https://doi.org/10.1099/0022-1317-40-3-531.
Islam, R., Salahuddin, M., Ayubi, M.S., Hossain, T., Majumder, A., Taylor-Robinson, A.W., Mahmud-Al-Rafat, A., 2015. Dengue epidemiology and pathogenesis: images of the future viewed through a mirror of the past. Virol. Sin. 30, 326–343. https://doi.org/10.1007/s12250-015-3624-1.
Jaworski, E., Routh, A., 2017. Parallel ClickSeq and nanopore sequencing elucidates the rapid evolution of defective-interfering RNAs in Flock House virus. PLoS Pathog. 13, e1006365. https://doi.org/10.1371/journal.ppat.1006365.
Jerzak, G.V.S., Bernard, K., Kramer, L.D., Shi, P.-Y., Ebel, G.D., 2007. The West Nile virus mutant spectrum is host-dependant and a determinant of mortality in mice. Virology 360, 469–476. https://doi.org/10.1016/j.virol.2006.10.029.
Juárez-Martínez, A.B., Vega-Almeida, T.O., Salas-Benito, M., García-Espitia, M., De Nova-Ocampo, M., Del Ángel, R.M., Salas-Benito, J.S., 2013. Detection and sequencing of defective viral genomes in C6/36 cells persistently infected with dengue virus 2. Arch. Virol. 158, 583–599. https://doi.org/10.1007/s00705-012-1525-2.
Junjhon, J., Pennington, J.G., Edwards, T.J., Perera, R., Lanman, J., Kuhn, R.J., 2014. Ultrastructural characterization and three-dimensional architecture of replication sites in dengue virus-infected mosquito cells. J. Virol. 88, 4687–4697. https://doi.org/10.1128/JVI.00118-14.
Kanthong, N., Khemnu, N., Pattanakitsakul, S.-N., Malasit, P., Flegel, T.W., 2010. Persistent, triple-virus co-infections in mosquito cells. BMC Microbiol. 10, 14. https://doi.org/10.1186/1471-2180-10-14.
Kanthong, N., Khemnu, N., Sriurairatana, S., Pattanakitsakul, S.-N., Malasit, P., Flegel, T.W., 2008. Mosquito cells accommodate balanced, persistent co-infections with a densovirus and Dengue virus. Dev. Comp. Immunol. 32, 1063–1075. https://doi.org/10.1016/j.dci.2008.02.008.
Karpf, A.R., Lenches, E., Strauss, E.G., Strauss, J.H., Brown, D.T., 1997. Superinfection exclusion of alphaviruses in three mosquito cell lines persistently infected with Sindbis virus. J. Virol. 71, 7119–7123.
Kim, D., Langmead, B., Salzberg, S.L., 2015. HISAT: a fast spliced aligner with low memory requirements. Nat. Methods 12, 357–360. https://doi.org/10.1038/nmeth.3317.
Kuno, G., 1982. Persistent infection of a nonvector mosquito cell line (TRA-171) with dengue viruses. Intervirology 18, 45–55.
Kuno, G., Oliver, A., 1989. Maintaining mosquito cell lines at high temperatures: effects on the replication of flaviviruses. Vitr. Cell. Dev. Biol. 25, 193–196.
Lee, E., Weir, R.C., Dalgarno, L., 1997. Changes in the dengue virus major envelope protein on passaging and their localization on the three-dimensional structure of the protein. Virology 232, 281–290. https://doi.org/10.1006/viro.1997.8570.
Li, D., Lott, W.B., Lowry, K., Jones, A., Thu, H.M., Aaskov, J., 2011. Defective interfering viral particles in acute Dengue infections. PLoS One 6. https://doi.org/10.1371/journal.pone.0019447.
Li, Y., Kim, Y.M., Zou, J., Wang, Q.-Y., Gayen, S., Wong, Y.L., Lee, L.T., Xie, X., Huang, Q., Lescar, J., Shi, P.-Y., Kang, C., 2015. Secondary structure and membrane topology of dengue virus NS4B N-terminal 125 amino acids. Biochim. Biophys. Acta 1848, 3150–3157. https://doi.org/10.1016/j.bbamem.2015.09.016.
Li, Y., Wong, Y.L., Lee, M.Y., Li, Q., Wang, Q.-Y., Lescar, J., Shi, P.-Y., Kang, C., 2016. Secondary structure and membrane topology of the full-length dengue virus NS4B in Micelles. Angew. Chem. Int. Ed. Engl. 55, 12068–12072. https://doi.org/10.1002/anie.201606609.
Manzano, M., Reichert, E.D., Polo, S., Falgout, B., Kasprzak, W., Shapiro, B.A., Padmanabhan, R., 2011. Identification of cis-acting elements in the 3′-untranslated region of the dengue virus type 2 RNA that modulate translation and replication. J. Biol. Chem. 286, 22521–22534. https://doi.org/10.1074/jbc.M111.234302.
Martin, M., 2011. Cutadapt removes adapter sequences from high-throughput sequencing reads. EMBnetjournal 17 (1), 10–12.
Martins, V.E.P., Alencar, C.H., Kamimura, M.T., Araújo, F.M., de, C., Simone, S.G.D., Dutra, R.F., Guedes, M.I.F., 2012. Occurrence of natural vertical transmission of dengue-2 and dengue-3 viruses in Aedes aegypti and Aedes albopictus in Fortaleza, Ceará, Brazil. PLOS ONE 7, e41386. https://doi.org/10.1371/journal.pone.0041386.
Matusan, A.E., Pryor, M.J., Davidson, A.D., Wright, P.J., 2001. Mutagenesis of the Dengue virus type 2 NS3 protein within and outside helicase motifs: effects on enzyme activity and virus replication. J. Virol. 75, 9633–9643. https://doi.org/10.1128/JVI.75.20.9633-9643.2001.
McMinn, P.C., Marshall, I.D., Dalgarno, L., 1995. Neurovirulence and neuroinvasiveness of Murray Valley encephalitis virus mutants selected by passage in a monkey kidney cell line. J. Gen. Virol. 76 (Pt 4), 865–872. https://doi.org/10.1099/0022-1317-76-4-865.
Miller, S., Sparacio, S., Bartenschlager, R., 2006. Subcellular localization and membrane topology of the Dengue virus type 2 Non-structural protein 4B. J. Biol. Chem. 281, 8854–8863. https://doi.org/10.1074/jbc.M512697200.
Milne, I., Bayer, M., Cardle, L., Shaw, P., Stephen, G., Wright, F., Marshall, D., 2010. Tablet—next generation sequence assembly visualization. Bioinformatics 26, 401–402. https://doi.org/10.1093/bioinformatics/btp666.
Modis, Y., Ogata, S., Clements, D., Harrison, S.C., 2003. A ligand-binding pocket in the dengue virus envelope glycoprotein. Proc. Natl. Acad.. Sci. USA 100, 6986–6991. https://doi.org/10.1073/pnas.0832193100.
Muñoz-Jordán, J.L., Laurent-Rolle, M., Ashour, J., Martínez-Sobrido, L., Ashok, M., Lipkin, W.I., García-Sastre, A., 2005. Inhibition of alpha/beta interferon signaling by the NS4B protein of flaviviruses. J. Virol. 79, 8004–8013. https://doi.org/10.1128/JVI.79.13.8004-8013.2005.
Newton, S.E., Short, N.J., Dalgarno, L., 1981. Bunyamwera virus replication in cultured Aedes albopictus (mosquito) cells: establishment of a persistent viral infection. J. Virol. 38, 1015–1024.
Osada, N., Kohara, A., Yamaji, T., Hirayama, N., Kasai, F., Sekizuka, T., Kuroda, M., Hanada, K., 2014. The genome landscape of the african green monkey kidney-derived vero cell line. DNA Res. 21, 673–683. https://doi.org/10.1093/dnares/dsu029.
Osuna-Ramos, J.F., Reyes-Ruiz, J.M., del Ángel, R.M., 2018. The role of host cholesterol during Flavivirus infection. Front Cell Infect. Microbiol 8. https://doi.org/10.3389/fcimb.2018.00388.
Perera, R., Kuhn, R.J., 2008. Structural proteomics of dengue virus. Curr. Opin. Microbiol. 11, 369–377. https://doi.org/10.1016/j.mib.2008.06.004.
Poirier, E.Z., Goic, B., Tomé-Poderti, L., Frangeul, L., Boussier, J., Gausson, V., Blanc, H., Vallet, T., Loyd, H., Levi, L.I., Lanciano, S., Baron, C., Merkling, S.H., Lambrechts, L., Mirouze, M., Carpenter, S., Vignuzzi, M., Saleh, M.-C., 2018. Dicer-2-dependent generation of Viral DNA from defective genomes of RNA viruses modulates antiviral immunity in insects (353-365.e8). Cell Host Microbe 23. https://doi.org/10.1016/j.chom.2018.02.001.
Pompon, J., Manuel, M., Ng, G.K., Wong, B., Shan, C., Manokaran, G., Soto-Acosta, R., Bradrick, S.S., Ooi, E.E., Missé, D., Shi, P.-Y., Garcia-Blanco, M.A., 2017. Dengue subgenomic flaviviral RNA disrupts immunity in mosquito salivary glands to increase virus transmission. PLoS Pathog. 13, e1006535. https://doi.org/10.1371/journal.ppat.1006535.
Randolph, V.B., Hardy, J.L., 1988. Phenotypes of St Louis encephalitis virus mutants produced in persistently infected mosquito cell cultures. J. Gen. Virol. 69 (Pt 9), 2199–2207. https://doi.org/10.1099/0022-1317-69-9-2199.
Reyes-Ruiz, J.M., Osuna-Ramos, J.F., Cervantes-Salazar, M., Lagunes Guillen, A.E., Chávez-Munguía, B., Salas-Benito, J.S., Del Ángel, R.M., 2018. Strand-like structures and the nonstructural proteins 5, 3 and 1 are present in the nucleus of mosquito cells infected with dengue virus. Virology 515, 74–80. https://doi.org/10.1016/j.virol.2017.12.014.
Rezelj, V.V., Levi, L.I., Vignuzzi, M., 2018. The defective component of viral populations. Curr. Opin. Virol. 33, 74–80. https://doi.org/10.1016/j.coviro.2018.07.014.
Riedel, B., Brown, D.T., 1977. Role of extracellular virus on the maintenance of the persistent infection induced in Aedes albopictus (mosquito) cells by Sindbis virus. J. Virol. 23, 554–561.
Roby, J.A., Pijlman, G.P., Wilusz, J., Khromykh, A.A., 2014. Noncoding subgenomic flavivirus RNA: multiple functions in West Nile virus pathogenesis and modulation of host responses. Viruses 6, 404–427. https://doi.org/10.3390/v6020404.
Routh, A., Head, S.R., Ordoukhanian, P., Johnson, J.E., 2015. ClickSeq: fragmentation-free next-generation sequencing via click ligation of adaptors to stochastically terminated 3′-azido cDNAs. J. Mol. Biol. 427, 2610–2616. https://doi.org/10.1016/j.jmb.2015.06.011.
Routh, A., Johnson, J.E., 2014. Discovery of functional genomic motifs in viruses with ViReMa-a Virus Recombination Mapper-for analysis of next-generation sequencing data. Nucleic Acids Res. 42, e11. https://doi.org/10.1093/nar/gkt916.
Salas-Benito, J.S., De Nova-Ocampo, M., 2015. Viral interference and persistence in Mosquito-Borne Flaviviruses. J. Immunol. Res. 2015, 873404. https://doi.org/10.1155/2015/873404.
Sánchez-Vargas, I., Scott, J.C., Poole-Smith, B.K., Franz, A.W.E., Barbosa-Solomieu, V., Wilusz, J., Olson, K.E., Blair, C.D., 2009. Dengue Virus Type 2 infections of aedes aegypti are modulated by the mosquito's RNA interference pathway. PLoS Pathog. 5, e1000299. https://doi.org/10.1371/journal.ppat.1000299.
Smith, K.M., Nanda, K., Spears, C.J., Ribeiro, M., Vancini, R., Piper, A., Thomas, G.S., Thomas, M.E., Brown, D.T., Hernandez, R., 2011. Structural mutants of dengue virus 2 transmembrane domains exhibit host-range phenotype. Virol. J. 8, 289. https://doi.org/10.1186/1743-422X-8-289.
Stanaway, J.D., Shepard, D.S., Undurraga, E.A., Halasa, Y.A., Coffeng, L.E., Brady, O.J., Hay, S.I., Bedi, N., Bensenor, I.M., Castañeda-Orjuela, C.A., Chuang, T.-W., Gibney, K.B., Memish, Z.A., Rafay, A., Ukwaja, K.N., Yonemoto, N., Murray, C.J.L., 2016. The global burden of dengue: an analysis from the Global Burden of disease study 2013. Lancet Infect. Dis. 16, 712–723. https://doi.org/10.1016/S1473-3099(16)00026-8.
Sun, Y., Jain, D., Koziol-White, C.J., Genoyer, E., Gilbert, M., Tapia, K., Jr, R.A.P., Hodinka, R.L., López, C.B., 2015. Immunostimulatory defective viral genomes from respiratory syncytial virus promote a strong innate antiviral response during infection in mice and humans. PLoS Pathog. 11, e1005122. https://doi.org/10.1371/journal.ppat.1005122.
Thenmozhi, V., Hiriyan, J.G., Tewari, S.C., Philip Samuel, P., Paramasivan, R., Rajendran, R., Mani, T.R., Tyagi, B.K., 2007. Natural vertical transmission of dengue virus in Aedes albopictus (Diptera: Culicidae) in Kerala, a southern Indian state. Jpn. J. Infect. Dis. 60, 245–249.
Tsai, K.-N., Tsang, S.-F., Huang, C.-H., Chang, R.-Y., 2007. Defective interfering RNAs of Japanese encephalitis virus found in mosquito cells and correlation with persistent infection. Virus Res. 124, 139–150. https://doi.org/10.1016/j.virusres.2006.10.013.
Vasilakis, N., Deardorff, E.R., Kenney, J.L., Rossi, S.L., Hanley, K.A., Weaver, S.C., 2009. Mosquitoes put the brake on arbovirus evolution: experimental evolution reveals slower mutation accumulation in mosquito than vertebrate cells. PLoS Pathog. 5, e1000467. https://doi.org/10.1371/journal.ppat.1000467.
Villordo, S.M., Filomatori, C.V., Sánchez-Vargas, I., Blair, C.D., Gamarnik, A.V., 2015. Dengue virus RNA structure specialization facilitates host adaptation. PLoS Pathog.

11, e1004604. https://doi.org/10.1371/journal.ppat.1004604.
Villordo, S.M., Gamarnik, A.V., 2013. Differential RNA sequence requirement for dengue virus replication in mosquito and mammalian cells. J. Virol. 87, 9365–9372. https://doi.org/10.1128/JVI.00567-13.
Wahid, S.F., Sanusi, S., Zawawi, M.M., Ali, R.A., 2000. A comparison of the pattern of liver involvement in dengue hemorrhagic fever with classic dengue fever. Southeast Asian J. Trop. Med. Public Health 31, 259–263.
Welsch, S., Miller, S., Romero-Brey, I., Merz, A., Bleck, C.K.E., Walther, P., Fuller, S.D., Antony, C., Krijnse-Locker, J., Bartenschlager, R., 2009. Composition and three-dimensional architecture of the dengue virus replication and assembly sites. Cell Host Microbe 5, 365–375. https://doi.org/10.1016/j.chom.2009.03.007.
WHO, 2009. Dengue: Guidelines for Diagnosis, Treatment, Prevention and Control: New Edition, WHO Guidelines Approved by the Guidelines Review Committee. World Health Organization, Geneva.
Yacoub, S., Wills, B., 2014. Predicting outcome from dengue. BMC Med. 12. https://doi.org/10.1186/s12916-014-0147-9.
Yap, T.L., Xu, T., Chen, Y.-L., Malet, H., Egloff, M.-P., Canard, B., Vasudevan, S.G., Lescar, J., 2007. Crystal structure of the dengue virus RNA-dependent RNA polymerase catalytic domain at 1.85-angstrom resolution. J. Virol. 81, 4753–4765. https://doi.org/10.1128/JVI.02283-06.
Yoon, S.W., Lee, S.-Y., Won, S.-Y., Park, S.-H., Park, S.-Y., Jeong, Y.S., 2006. Characterization of homologous defective interfering RNA during persistent infection of Vero cells with Japanese encephalitis virus. Mol. Cells 21, 112–120.
Zou, J., Xie, X., Wang, Q.-Y., Dong, H., Lee, M.Y., Kang, C., Yuan, Z., Shi, P.-Y., 2015. Characterization of dengue virus NS4A and NS4B protein interaction. J. Virol. 89, 3455–3470. https://doi.org/10.1128/JVI.03453-14.